



# Cut-off lows in the Southern Hemisphere and their extension to the surface

Michael A. Barnes<sup>1,2</sup> · Thando Ndarana<sup>2</sup> · Willem A. Landman<sup>2</sup>

Received: 21 June 2020 / Accepted: 18 January 2021 / Published online: 9 February 2021  
© The Author(s), under exclusive licence to Springer-Verlag GmbH, DE part of Springer Nature 2021

## Abstract

Many cut-off low (COL) climatologies have been done throughout the Southern Hemisphere. Few have focused on COL vertical depth and their link to surface cyclones that often accompany these systems. Here we extend these climatologies in order to gain an understanding of the spatial, mobility, temporal, and seasonal variability of COL extensions towards the surface. Deep COLs (dCOLs), with extension all the way to the surface, are most frequent in the autumn months, are longer lasting, are more mobile and found most frequently situated in the high latitudes. They are usually collocated with Rossby wave breaking (RWB) on multiple isentropic surfaces. These RWB events drive high potential vorticity air into the upper troposphere. The depths of these intrusions are also shown to be critical to the development of COL extensions with dCOLs associated with deeper intrusions into the mid-troposphere. Upper-level PV features are collocated with warm surface potential temperature anomalies which can play a critical role in surface cyclogenesis. The warm surface potential temperature features, when out of phase with coupled upper tropospheric processes (surface features lagging behind upper level processes), can inhibit surfaceward extension and result in shallow COL (sCOL) development. Composite analysis shows that dCOLs that drive their own surface low development result in the simultaneous amplification of troughs throughout the troposphere, with the surface cyclone developing within a day of the COL.

**Keywords** Cut-off low extensions · Surface cyclogenesis · Potential vorticity · Rossby wave breaking · Stratospheric intrusions

## 1 Introduction

Cut-off lows (COLs) are a cold-cored, closed, upper-air low pressure systems (Nieto et al. 2005) that develop by becoming displaced equatorward out of the westerly jet in the extra-tropics (Palmén 1949; Palmen and Newton 1969). They usually persist for up to 4 days (Singleton and Reason 2007a), but can on occasion last longer. Over South Africa, COLs contribute significantly to the overall rainfall of the country, especially during the spring and autumn months (Favre et al. 2013). They are also a major contributor of extreme rainfall events particularly over the southern and

eastern parts of the country. In fact, COLs contribute to 16% of the total annual rainfall of the cape south coast (Engelbrecht et al. 2015). In addition, deep moist convection taking place within COLs can produce short bursts of extreme rainfall leading to 20% of all flash-flooding events over South Africa (Singleton and Reason 2007a).

Various Southern Hemispheric COL climatologies have been completed focussing on COLs on different geopotential levels. Many have defined COLs as closed circulations at the 500 hPa level (Fuenzalida et al. 2005), whilst others use levels between 200 and 300 hPa (Nieto et al. 2005; Singleton and Reason 2007b; Ndarana and Waugh 2010; Pinheiro et al. 2019). Muñoz et al. (2020) compared the climatologies and found that whichever the level COLs are studied, their features remain consistent. There are four stages in the life cycle of COLs (Nieto et al. 2005). First, an upper level trough develops coincident with a temperature wave situated to the west of the geopotential wave. During this stage, lower tropospheric cold air advection into the centre of the trough results in the amplification of the geopotential and

✉ Michael A. Barnes  
weathermanbarnes@gmail.com;  
michael.barnes@weathersa.co.za

<sup>1</sup> Marine Research Unit, South African Weather Service, Cape Town, South Africa

<sup>2</sup> Department of Geography, Geoinformatics and Meteorology, University of Pretoria, Pretoria, South Africa

temperature waves. As the amplitude continues to increase, it starts to detach from the westerly jet. This is the second stage known as the tear-off stage. Eventually, the cold air that has penetrated the centre of the deep trough gets cut-off equatorward from the extratropics. This third stage is known as the cut-off stage of COL development. In the final stage, the COL dissipates and usually merges again with a trough in the westerly zonal jet. In the tropics, the movement of COLs is however more erratic where COLs can retrograde (move in a westerly direction) or decay with equatorward trajectory (Favre et al. 2013), not re-merging with the westerly zonal jet.

The dynamics of upper tropospheric cyclonic circulations have been studied in the Northern Hemisphere since the late 1940s. A first detailed account of COLs was done by Palmén (1949) who showed a case of an upper-level trough deforming and amplifying, with the cold airmass becoming cut off from the polar airmass. The case study detailed the lowering of the tropopause and how strong upper tropospheric convergence and associated subsidence leads to an increase in relative vorticity and upper level cyclonic development. The development of these systems was also theorised to be sustained by the amount of relative vorticity of the upper level cyclone, with increased cyclonic motion resulting in COLs extending towards the surface (Hsieh 1949). Early studies also showed the extension of isentropic potential vorticity (PV) values well into the mid-levels of the troposphere during these intense COL events. This led to the theory presented by Kleinschmidt (1950) that these high-PV stratospheric intrusions in fact induce the cyclonic circulation of the COL (Bell and Bosart 1993). This theory has now formed the basis of the “Isentropic PV Thinking” methodology of dynamical analysis which was later reinvigorated in the landmark paper by Hoskins et al. (1985) and has continued to be used in contemporary studies in dynamic meteorology (e.g., Holton and Hakim 2013; Lackmann, 2011).

Isentropic PV thinking is based around the invertibility principle (Hoskins et al. 1985). The invertibility principle states that if PV on each isentropic surface including that of the lower boundary is known, then all other meteorological fields (geopotential height, temperature and horizontal velocity) can be calculated under a suitable balance condition. Isentropic PV fields can therefore be used to describe the evolution of all other dynamical fields. Since PV is conserved for flow that is adiabatic and frictionless, PV frameworks are extremely useful for studying dynamical processes including that of COLs. COLs are known to be linked with high-PV anomalies (Bell and Bosart 1993; van Delden and Neggers 2003; Nieto et al. 2005). High-PV values are negative in the Southern Hemisphere and positive in the Northern Hemisphere. These anomalies are the result of intrusions of high-PV stratospheric air transported isentropically and equatorward into the upper troposphere (Hoskins

et al. 1985). Theoretical analyses of PV show that positive PV anomalies in the upper troposphere can be viewed from a cross-sectional point of view as surfaceward bends in the dynamical tropopause (Hoskins et al. 1985). The region of higher PV air than that of the air surrounding it results in cyclonic circulation around the high-PV anomaly.

Further, Rossby-wave breaking (RWB) events have also been well established to result in similar high-PV anomalies in the troposphere. RWB, defined as the rapid and irreversible deformation of PV contours (Mcintyre and Palmer 1983), have been linked with the formation of COLs in many observational studies (e.g., Baray et al. 2003). Most recently, a climatological link has been established between COLs and RWB events in the Southern Hemisphere (Ndarana and Waugh 2010). 89% of the COLs identified using National Centers for Environmental Prediction/National Center for Atmospheric Research (NCEP/NCAR) reanalysis data (Kalnay et al. 1996) were associated with RWB events. The remainder, although not being associated with RWB, were still associated with PV intrusions from the stratosphere. RWB events along lower isentropic surfaces have also been shown to correspond to COLs closer to the surface (500 hPa), with RWB on higher surfaces corresponding to COLs nearer the tropopause (Ndarana and Waugh 2010).

Stratospheric-tropospheric exchanges have also been well linked with cyclogenesis at the surface. An early observational study on the President’s Day cyclone of 1979 in the United States of America showed an example of an explosive surface cyclone that was associated with a deep stratospheric event (Uccellini et al. 1985). In this case high-PV values were observed close to the 700 hPa level. Similar observational studies have also been conducted in the South Atlantic (Funatsu et al. 2004; Iwabe and Da Rocha 2009). The focus of observational studies has resulted in the PV-tower theory. PV towers are defined as the vertical alignment of three distinct PV anomalies in the upper troposphere, lower troposphere and at the surface (Čampa and Wernli 2012; Pang and Fu 2017). These PV anomalies govern the evolution and development of the surface cyclone by resulting in deep cyclonic circulation throughout the troposphere. Čampa and Wernli (2012) have also shown the importance of all three of these anomalies in the maturing and deepening of explosive cyclones. Notably, in weaker cyclones, low-level and surface anomalies are weaker. This suggests the importance of upper level process in the development of closed surface circulations, with low-level and surface anomalies working in unison with upper level processes to evolve the surface circulations.

Some COL climatologies have provided some insight into the number of COLs that are associated with surface cyclones. In the Northern Hemisphere, 47.1% of COLs were found to be associated with surface cyclones and a high-PV anomaly at the 330 K surface (Nieto et al.

2005). In the Mediterranean, 60% of COLs were found to extend to the surface using a low-pressure minimum detection algorithm (Porcù et al. 2007). 38% of COLs in the Mediterranean study were found to have a surface cyclone that was vertically related to the COL. Recently, in the Southern Hemisphere, a COL climatology using a relative vorticity tracking algorithm found that 19.4% of COLs have a vertically related surface cyclone, with 65% of intense COLs associated with a surface low pressure system (Pinheiro et al. 2020). A regional study over the southern parts of South America have also shown that 25% of COLs detected were associated with surface cyclones using a subjective algorithm over a 10 year period (Campetella and Possia 2007).

Although surface cyclogenesis has been studied extensively in a PV framework, the focus of these studies has been on explosive cyclogenesis events. Explosive cyclogenesis events are important due to the large impact they can have on local communities resulting in extreme precipitation events and windstorms (Liberato 2014; Barnes et al. 2021) as well as large wave and storm surge events (Rautenbach et al. 2020). Few studies have focussed on the development of generic surface lows that are dynamically driven by upper tropospheric processes. The climatological variability of Southern Hemispheric of COL extensions is still an open question. In this study, we thoroughly study Southern Hemisphere COL extensions to the surface in a climatological setting. In conjunction with this database, the number of COLs that are associated with closed surface low pressures are studied. COLs and surface low pressures can also be linked to RWB. RWB is a well-known driver of stratospheric intrusions which in turn can result in cyclonic circulations. RWB-COL linkage statistics are also presented to corroborate the findings of Ndarana and Waugh (2010) with a different reanalysis dataset. PV diagnostics are performed to determine the effect that the depth of stratospheric intrusions has on the development of surface low pressures associated with COLs. Composite analysis of various fields (geopotential height, PV and potential temperature) provide insight into the general behaviour of COLs that extend to the surface and those that do not.

This paper is organised as follows. Section 2 provides a summary of the data used in the analysis. All the algorithms and diagnostic methods are also fully described. The results of the statistical analyses are presented in Sect. 3. This section is divided into a general summary of the statistics of COL and COL depth databases with respect to the variability of extensions, a summary of the linkage statistics of the RWB and COLs detected and an analysis of the PV diagnostic and composite analyses. Conclusions are drawn and discussed in Sect. 4.

## 2 Data and algorithms

### 2.1 Data

In this study, 40 years (1 January 1979–1 January 2019) of European Centre for Medium-Range Weather Forecasting (ECWMF) Reanalysis (ERA-Interim) data (Dee et al. 2011) are used. All fields used have a  $2.5^\circ \times 2.5^\circ$  horizontal resolution and a temporal resolution of 6 h. Although data from the ERA-Interim dataset has a spatial resolution of  $0.75^\circ \times 0.75^\circ$ , the lower resolution dataset is used for computational efficiency of the algorithms. This resolution is sufficient for this work since all processes such as COLs are of a synoptic scale (600–1200 km) and therefore are detectable in the lower resolution data (Fuenzalida et al. 2005; Ndarana and Waugh 2010; Reboita et al. 2010). A variety of variables on various levels are used throughout the study. Each of these levels and variables are explained as they are used in each algorithm and section.

### 2.2 COL detection algorithm

A database of COLs between 1979 and 2018 is produced from ERA-Interim  $2.5^\circ$  data. COLs in this database are defined on the 250 hPa geopotential height level at 6-hourly intervals. Although some studies use various levels to define COLs in various COL climatologies (e.g., Fuenzalida et al. 2005; Nieto et al. 2005; Reboita et al. 2010), the 250 hPa level is chosen as it represents the vertical position of both the subtropical and mid-latitude dynamical tropopause (Ndarana and Waugh 2010). This is important as this study aims at linking upper tropospheric processes to the extension of COLs to the surface. The COL detection algorithm used in this study is based on a similar COL detection algorithm used by Ndarana and Waugh (2010) and is a geopotential-based tracking algorithm. Most climatologies use geopotential tracking methodologies for COL climatologies (Muñoz et al. 2020). Other authors use PV frameworks for the detection of COLs (Sprenger et al. 2007). However, a geopotential-based algorithm was chosen here to maintain the COL database's independence from PV since we will later look at their relation to stratospheric intrusions of high-PV. The geopotential framework is quasi-horizontal. This has the disadvantage of not sloping with the dynamical tropopause and thus some COL events may be missed. However, the quasi-horizontal, geopotential framework is also more readily used by operational users and therefore a geopotential height detection algorithm and subsequent analysis are more beneficial to operational meteorologists. The algorithm to detect COL centres is described in detail

below and for ease of reference, a schematic of these steps for COL detection are provided visually in Fig. 15 in the “Appendix”.

*Step 1:* 250 hPa contours at a 1 geopotential meter (gpm) interval are derived at each timestep (6 h). 1gpm is chosen for computational efficiency of the algorithm but with enough resolution to detect a closed low as soon as it has formed. All contours that are closed (with identical start and end points) are then detected. Finally, the geometric centre of each of these closed contours is obtained and saved into the database as potential COL points.

*Step 2:* Only COL points between 50° S and 15° S are retained in the COL point database. Tropical lows are excluded by excluding lows north of 15° S. This has been a standard practice in many COL climatologies (e.g., Fuenzalida et al. 2005) eliminating lows anywhere from 10° S to 20° S. Lows are excluded below 50° S to exclude polar lows from the database which are not detached from the polar regions (Muñoz et al. 2020).

*Step 3:* All high-pressure closed contour centres are then filtered out by applying a geopotential height condition onto each COL point in the database. First, the nearest grid point to the COL point is detected. COL points are filtered out if the nearest grid point to the COL point is lower than six neighbouring of the possible eight grid points by at least 10gpm. This condition has been used in multiple COL climatologies (e.g., Nieto et al. 2005; Porcù et al. 2007).

*Step 4:* COLs, by definition, need to be fully detached from the westerly wind belt. A zonal wind direction condition is used to apply this condition. A COL point is filtered out of the database if the closest grid point to the COL point and/or the grid point to the south of this grid point has a easterly component. It has been shown that using a single point detection methodology could result in an overestimation of COLs (Pinheiro et al. 2019). This risk is however removed by including a closed contour condition (as performed in Step 1) together with a single point wind condition, as together they imply total cyclonic wind flow.

*Step 5:* COLs are cold-cored systems and therefore a cold-core condition is applied to the database as has been used in many previous COL climatologies (e.g., Nieto et al. 2005; Reboita et al. 2010). In this study, the cold core condition is applied by detecting 250-500 hPa local thickness minima. Thickness fields are used as they provide a better representation of the thermal properties of the layer (Ndarana and Waugh 2010). A COL point in the database is said to have been associated with a cold core if the thickness of the nearest grid point to the COL point is less than at least five of its eight nearest neighbours. COL points that do not meet this condition are discarded from the database.

*Step 6:* The database now contains multiple COL points, many of which belong to the same COL, since rings of multiple closed contours would have been identified in Step 1.

COL points that share a 10-by-10-degree area are deemed to belong to the same COL. The point within this box with the lowest central 250 hPa geopotential height is deemed to be the COL point with the remainder of the COL points filtered out of the database.

*Step 7:* Randomly sampled, subjective analysis of the COLs identified at the end of Step 6 reveals that COLs are intermittently identified with some timesteps within a COL trajectory missing from the database. This would result in COL trajectories being split into multiple trajectories and an over-estimate of individual COLs in the database. This issue was also previously noted by Porcù et al. (2007). Many studies do not have this issue as many use daily averaged data (e.g., Nieto et al. 2005; Ndarana and Waugh 2010). This problem was previously solved by filling “gaps” in a COL’s trajectory subjectively (Porcù et al. 2007). A COL trajectory was deemed to have a gap if there were no more than two consecutive missing six-hourly detections. In this study, this same technique is applied objectively. A database of simple closed low pressures is gathered using steps 1–3. If a “gap” of no more than 2 timesteps is detected in a COL, the gap is filled with a detected low-pressure centre within a 5°×5° range of the previous COL centre, if it existed. This step results in grouping COLs points that are part of the same COL system trajectory. Although the size of the 5°×5° search box in meters is different between the tropics (close to 15° S) and the extratropics (close to 50° S), this is deemed to be sufficient since very few COLs travel fast enough such that the COL point will not be contained in the search box at the subsequent timestep (Reboita et al. 2010). Additionally, it has been shown that the zonal mean velocity of COLs is greater towards the poles (Pinheiro et al. 2017) and therefore an increased size search box (in terms of meters) at the poles is in fact appropriate.

*Step 8:* Finally, a longevity condition is imposed on the COL trajectories in the database. COLs that are not present at four consecutive timesteps (24 h) are removed from the database.

### 2.3 COL vertical structure algorithm

A COL vertical extension study of the Mediterranean is used as a basis for COL vertical structure methodology applied here (Porcù et al. 2007). First, a 5×5 grid-point area is extracted from around the COL grid cell. Low pressure regions at various geopotential height levels are detected. A grid point is considered to be a low-pressure minimum if six or more out of the eight of its neighbouring grid cells are lower than the threshold specified for that particular level. Specified level thresholds are obtained by Porcù et al. (2007) who used smoothly decreasing values from 10 gpm at 200 hPa to 2 gpm at 1000 hPa. These values represent 30% of the standard deviation of the geopotential height

distribution amongst neighbouring grid points. In the event that more than one low pressure minimum is detected for a COL point at a specific timestep, the coordinates of the low-pressure minimum with the lowest geopotential height is chosen and recorded in the low-pressure minimum database for that particular level.

From this detection methodology, a low-pressure minimum database at each level below the COL and time is created throughout the trajectory of the COL. Although each low-pressure minimum was detected in the region of each COL point, the search is performed independently of the levels above and below it. If a low point was detected at the 300 hPa level below a COL point in the COLs trajectory, it is deemed to have a depth of 300 hPa. If the COL reached a depth of 300 hPa, the search is repeated at the level below. This process is further repeated for all the levels down to the surface at 1000 hPa. The COL depth is defined as the minimum depth at which a low is present in the COL point zone throughout the life of the COL.

An independent surface low pressure database is derived to analyse whether a closed and defined surface cyclone is collocated with a detected COL. Surface low pressure minima are detected using a similar procedure to steps 1–3 of the COL detection algorithm as defined in Sect. 2.2. Mean sea level pressure data is used to find closed contours. Closed contours are detected at 1 hPa interval. Low pressures are isolated from high pressure closed contours by using the nearest neighbour methodology as before but using a neighbourhood threshold of 2 hPa.

## 2.4 Classification of COLs in terms of their depth

For simplicity in analysing the results of COL depths we classify COLs into two groups. *Deep COLs* (dCOLs) refer to COLs which have a depth down to 1000 hPa. A *shallow COL* (sCOL) will refer to a COL with a depth 500 hPa or shallower. To determine the relationships between COLs and surface cyclones, we use a method similar to that described by Porcù et al. (2007). An independent surface low pressure database is created using mean sea level pressure (MSLP) as described in Sect. 2.3. Similarly to Porcù et al. (2007), we define the following classification of COL and surface low relationships:

- COLs are separated into deep COLs (*dCOLs*) and shallow COLs (*sCOLs*). dCOLs refer to COLs which have a depth down to the surface at 1000 hPa (as detected by the algorithm in Sect. 2.3) whilst *sCOLs* will refer to a COL with a depth 500 hPa or shallower.
- dCOLs are separated into COLs that are associated with a surface low (*type 1 dCOLs* or *d1COLs*) from the independently derived surface low database (as defined in Sect. 2.3) and those that are not (*type 2 dCOLs* or *d2COLs*). A dCOL is said to be associated with a surface low if the independently detected surface low is found within a  $5^\circ \times 5^\circ$  area of the COL point during any time during its trajectory. Since the COLs in this class have already been defined as deep, extending all the way to the surface, the associated low is also vertically related to the COL. This classification differentiates deep-COLs with a distinct surface low-pressure cell at the surface (in which a closed surface low is found on the MSLP surface) from deep-COLs with a weak cyclonic circulation at the surface (in which a low pressure minimum is found at 1000 hPa but without closed cyclonic circulation).
- d1COLs are then separated by their temporal relation to their accompanying surface cyclone. d1COLs are classified into COLs whose surface cyclones formed at or after the first detected point in the COLs life cycle (*type 1a dCOLs* or *d1aCOLs*) and those formed before the COL developed (*type 1b dCOLs* or *d1bCOLs*). This classification aims at determining the number of surface lows that develop as a result of the mechanisms that result in the COLs development versus the number of COLs that move over already pre-existing low-pressure zones or cells. The upper level dynamics associated with the development of a COL can result in the development of closed cyclonic circulation at the surface prior to the closed circulation in the upper levels (associated with the COL) as seen in the case study by Barnes et al. (2021). Even though the surface circulation may develop first, it results from the same mechanism that resulted in the COL's development and therefore can still be considered as part of the same system. Therefore, in order to include these processes, surface lows that developed up to 12 h before the COL are included in type 1a dCOLs (d1aCOLs).

## 2.5 RWB detection algorithm

RWB events are identified using the geometry of their overturned PV features on isentropic surfaces (e.g., Barnes and Hartmann 2012; Esler and Haynes 1999; Ndarana and Waugh 2011). In this study we employ the RWB identification methodology similar to that of Ndarana and Waugh (2011) and Barnes and Hartmann (2012) based on the geometric properties of PV contours. Isentropic PV can be expressed mathematically by:

$$PV = -g(\zeta_\theta + f) \frac{\partial \theta}{\partial p},$$

with  $\zeta_\theta$  the relative vorticity on an isentropic surface,  $f$  the Coriolis parameter,  $\theta$  the potential temperature and  $p$  the pressure. The southern (northern) hemispheric stratosphere

is associated with larger negative (positive) PV values. The PV contours of  $-1.5$ ,  $-2$  and  $-2.5$  PVU (PV units,  $1 \text{ PVU} = 10^{-6} \text{ km}^2 \text{ s}^{-1} \text{ kg}^{-1}$ ) on the 315-, 320-, 330- and 350-K isentropic surfaces are used. The dynamical tropopause varies with height both seasonally where it is closer to the surface in winter and latitudinally where it is closer to the surface nearer the poles (Kunz et al. 2011; Ndarana and Waugh 2011). The choice of the set of isentropic levels considered here are coincident with the dynamical tropopause taking into account the tropopause height variability between different seasons and latitudes (Ndarana and Waugh 2011, Figure 1) from the available isentropic levels in the ERA-Interim dataset. At each level, contours are found for each of the specified contour intervals. We first eliminate all PV cut-offs and small-scale features by eliminating all contours that have fewer points than the longitude grid (144). Once the large-scale PV contours have been isolated, overturning features of each contour are identified. A contour is considered to be overturned if a longitudinal line intersects the contour two or more times. This is done at a zonal resolution of  $1^\circ$ . At each longitude where the contour is intersected more than twice, the coordinates of the most northerly and most southerly intersecting coordinates are recorded. Consecutive overturned longitudinal sections are then

considered as part of the same RWB event. RWB events are recorded as closed polygons whose bounds are the upper and lower coordinates recorded by the algorithm. Small-scale RWB events are filtered by only adding RWB events whose overturning area has a span of at least  $10^\circ$  to the database. Finally, we filter out areas of the RWB polygons which intersect areas by which  $\partial_y PV > 0$ . This results in intrusions in which overturning does not take place being removed from the database. Each polygon is recorded with its associated timestep, isentropic level and PV contour interval.

## 2.6 Stratospheric depth algorithm

Stratospheric depth changes associated with intrusions are mapped to correlate with the depth of each COL. The stratosphere is well known to be associated with high-PV air (Holton and Hakim 2013). Using this fact, stratospheric air can be mapped and differentiated from low-PV tropospheric air. In order to find these intrusions of high-PV air, the algorithm described by Sprenger (2003) and later improved by Škerlak et al. (2014) is employed. The algorithm makes use of a labelling system differentiating the five different airmasses as shown in the schematic in Fig. 1 of Škerlak et al. (2014). The algorithm is run on ERA-Interim data for the Southern

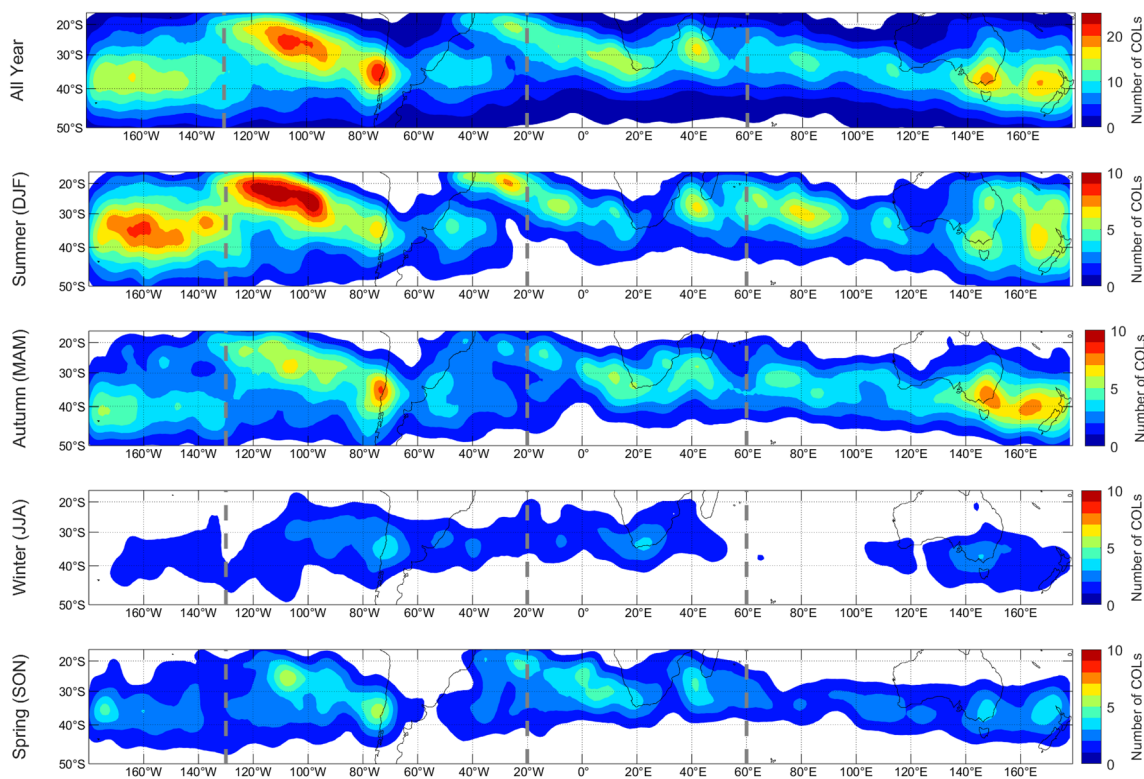


**Fig. 1** COL densities of all points in the COL database. COL points are gridded into  $1^\circ \times 1^\circ$  bins and smoothed using a  $5^\circ \times 5^\circ$  gaussian filter. Annual (top panel) and seasonal distributions are provided.

Grey dashed lines denote the South American, African and Australia–New Zealand sectors as used throughout this study

Hemisphere north of 65° S using PV values for levels between 50 and 1000 hPa at a vertical resolution of 50 hPa. The stratosphere is initiated at 30 hPa with each value given the label 2 indicating that stratospheric air is present. For the purposes of this study, a value of  $-1.5$  PVU is deemed to be the dynamical tropopause. Although  $-2$  PVU is often used to represent the dynamical tropopause, the  $-1.5$  PVU contour is chosen as PV contours closer to the surface are more sensitive and variable in the vertical whilst still being representative of the dynamical tropopause. This allows for a clearer diagnosis of the depth of the intrusion compared to more stratospheric contours. Using a stratospheric PV value of  $-1.5$  PVU, a value is given the label 2 (indicating stratospheric air), if it has a PV value of less than  $-1.5$  PVU and it has a neighbour either horizontally, vertically or diagonally that is also stratospheric air (label 2). If a grid cell has a value of less than  $-1.5$  PVU and it does not have a label 2 neighbour, it is labelled as a label 3 indicating a high-PV stratospheric cut-off or low-level high-PV feature. If the grid cell is greater than  $-1.5$  PVU, it is considered to be tropospheric air and given a label 1. Furthermore, tropospheric cut-offs (grid cells with PV greater than  $-1.5$  PVU) that are completely surrounded by stratospheric air are given the label 4. Finally, high-PV values can also be associated with very stable surface layers, especially over the polar regions (Škerlak et al. 2014). These surface-bound high-PV values (high-PV values that are in contact with the surface but not in contact with the stratosphere) are differentiated from stratospheric blobs and are given the label 5.

## 3 Results

### 3.1 COLs and extended COLs in the Southern Hemisphere

Using the algorithm in Sect. 2.2, a total of 10,543 COL trajectories were identified in the Southern Hemisphere. This represents an average of about 258 COL events per year. A summary of these events in the form of a density map is shown in Fig. 1. The density map of COL points is created by gridding all the COL points in the database into  $1^\circ \times 1^\circ$  bins and smoothing the binned data using a  $5^\circ \times 5^\circ$  gaussian filter. The densities obtained mirrors COL climatologies in previous studies. High densities are shown to the west of the Andes and the African continents as well as in the Tasman Sea. The effect of topography can be seen with high COL density areas found to the west of mountainous areas such as the Andes, New Zealand Alps and African Plateau promoting upper-level cyclolysis on the leeward side and cyclogenesis on the upstream side of these features (Fuenzalida et al. 2005). Average annual COL numbers found are also in the range of other Southern Hemisphere climatologies (Reboita

et al. 2010; Pinheiro et al. 2017, 2019). It is however a significant rise in COLs found in some studies. Ndarana and Waugh (2010) found only 81 COLs per year at the 250 hPa level. The study however used NCEP/NCAR reanalyses data. It has however been shown that significant differences can occur between COL climatologies using European Centre for Medium-Range Weather Forecasts Re-Analysis (ERA)-40 and NCEP/NCAR (Reboita et al. 2010). In fact, climatologies over the Southern Hemisphere using ERA reanalysis can detect up to double the amount of COLs using the same algorithm, depending on the level.

#### 3.1.1 A Southern Hemispheric climatology of extended COLs

The COL depth as defined in Sect. 2.3 is calculated in order to determine the lowest depth that the upper level low pressure system attained during its life cycle. The Southern Hemispheric COL depths are shown in Fig. 2. 57.8% of the COLs in the Southern Hemispheric database reached the surface (1000 hPa level), with only 31.6% and 38.7% reaching the 500 hPa and 600 hPa levels respectively. This is consistent with the findings of Porcù et al. (2007) in the Mediterranean region. Few COLs are very shallow, but generally COLs extend into at least the mid-troposphere (400–600 hPa). Interestingly, very few COLs extend down to the 700–925 hPa level that do not extend all the way to the surface. This “gap” in the COL depth does differ from the results in the Mediterranean study (Porcù et al. 2007). Although the number of Mediterranean COLs gradually increases to the 500 hPa level as is found in the Southern Hemisphere, the number of COLs extending below the 500 hPa level do not decrease sharply in the Mediterranean. Instead the number of Mediterranean COLs reaching the 700–850 hPa levels were found to be comparative to the number of COLs extending to the mid-levels. It has been shown that more intense cyclones over the Mediterranean region are generally associated with lesser diabatic-induced low-level PV structures compared to that of the surrounding larger ocean basins of the Northern Hemisphere such as the Atlantic and Pacific (Čampa and Wernli 2012). As the Southern Hemispheric region studied here is similar to the large oceanic basins, this boost in low-level PV could result in more of the extensions that extend into the low-levels reaching all the way to the surface. In addition, cyclone tracking is a challenge in the Mediterranean region due to the complex topography and stark contrast between the sea and surrounding land (Flaounas et al. 2015). This could indicate that some surface-level low-pressure minima could have been missed in the Mediterranean study enhancing the number of COLs that extend to the low-levels but do not extend to the surface. The results for the COL depth analysis throughout the southern African, Australia–New Zealand

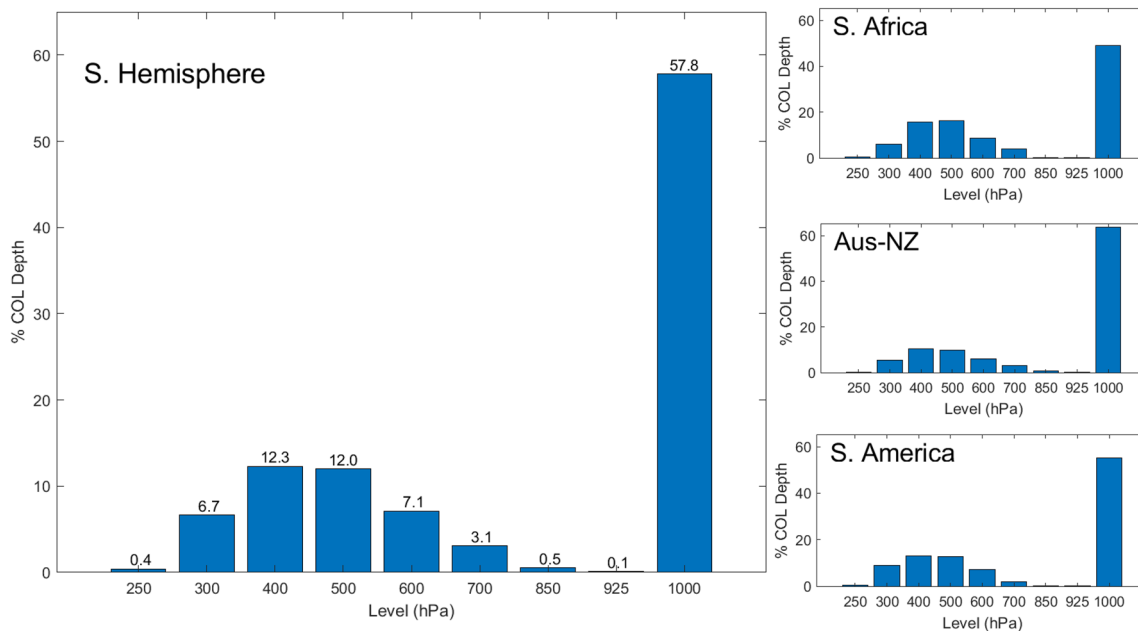


**Fig. 2** Lowest level in which a low-pressure centre could be detected beneath a detected COL (250 hPa). Results for the entire Southern Hemisphere (left) as well as the southern African, Australia–New Zealand and South American subregions (right) are shown

and South American sectors as shown in Fig. 1 and will be discussed fully in Sect. 3.1.2.

COL depths give a sense of the COLs that extend fully to the surface. However, COLs also exist in conjunction with closed surface lows. This was observed to have occurred during various observational studies (Uccellini et al. 1985; Iwabe and Da Rocha 2009; Barnes et al. 2021). The classification of COL depths in relation to the type of circulation at the surface as defined in Sect. 2.4, is used to analyse COL extensions. As shown in Fig. 2, dCOLs make up 57.8% of the COLs in the Southern Hemisphere, with sCOLs making up only 31.4%. The classification process found that of the dCOLs, the majority (89.5%) are associated with closed low-pressure circulations at the surface (d1COLs). The remainder of the dCOLs (10.5%) do present with surface low pressure minima (i.e., a surface trough), but have no associated defined, closed cyclonic circulation.

Further classifying these d1COLs reveals that a larger proportion of these low-level circulations developed from 12 h before the development of the COL. In fact, 53.1% of the d1COLs are classified as type 1a dCOLs (d1aCOLs) with the remainder of the lows developing before initial detection the COL (d1bCOLs). These results show that although the mechanisms that drive COL development can result in the development of surface cyclonic circulations, COLs can also develop in areas where these circulations already exist. The processes that result in the COLs surfaceward extension still influences the low-pressure system at the surface even if it is formed before the COL develops. The upper level

processes together with surface level processes can result in a deepening of the surface cyclones. In fact, in the Southern Hemisphere, 78.4% of the d1bCOLs were associated with a decrease in the 1000 hPa geopotential minima identified from the start of the COLs lifecycle. Half of the d1bCOLs showed significant decreases of over 20 gpm in the 1000 hPa geopotential minima.

### 3.1.2 Spatial variability of extended COLs within the Southern Hemisphere

The analysis performed in Sect. 3.1.1 is repeated for specified sectors of the Southern Hemisphere. The sectors studied are the southern African sector (20° W to 60° E), the Australian–New Zealand sector (60° E to 130° W) and the South America sector (130° W to 20° W). The largest sector, the Australia–New Zealand sector, is the most active COL sector with nearly half of the COLs (5026 COLs, 125 COLs per year) in the database located in this sector. Comparatively the smallest sector, the southern African region is the least active sector with 2290 COLs (57 COLs per year) whilst 3613 COLs (90 COLs per year) are identified in the South American sector. The distribution of COLs between the three sectors is consistent with previous studies (Fuenzalida et al. 2005; Reboita et al. 2010). The variations in the distributions of COLs are likely the result of the variability and preferred position in RWB events (Ndarana and Waugh 2011) and orographic effects (Fuenzalida et al. 2005). COL depths for the three sectors



are shown in Fig. 2. The COL depth distributions in each of the three sectors are relatively consistent with results for the entire hemisphere. Very few COLs extend to the low-levels that do not extend fully to the surface. The southern African sector contains the lowest ratio of dCOLs with 49% of the COLs extending all the way to the surface. This region also comprises of more sCOLs than the other two sectors with 38.3% of the COLs extending to only the 500 hPa level. Conversely the Australia–New Zealand sector is the most active in terms of dCOL development with 63.6% of the COLs extending to the surface.

Despite the differences in the ratio of sCOLs to dCOLs in each sector, the percentage of dCOLs associated with defined cyclonic surface circulation remains consistent throughout all three sectors. 89–90% of the dCOLs in each sector are classified as d1COLs. The southern African sector stands out in terms of the temporal relationship between the COL and the surface low. This sector comprises of slightly more dCOLs which develop their own surface circulations than the other two sectors. In the southern African sector, 57.4% of the d1COLs developed surface low pressure cells near or after the development of the COL compared to 52.3% and 51.5% in the Australia–New Zealand and South American sectors respectively. A summary of the results of the classified COLs for both the Southern Hemisphere and all three of the sectors are given in Table 1.

Another notable characteristic difference between dCOLs and sCOLs is the distinct latitudinal discrepancy between the two different types. The distribution of all dCOL and sCOL points in the database with latitude are shown in Fig. 3. From the COL point distributions, it is clearly visible that sCOLs are more often found in the subtropics (north of 30° S), whilst dCOLs are generally found towards the extratropics (south of 30° S). Of all detected sCOLs within the Southern Hemisphere, 77.2% of sCOLs contained tracks north of the 30° S line. Only 22.5% of the dCOLs are found to have crossed the 30° S latitude line. Conversely, 92.6% of all dCOLs had at least one point south of the 30° S line. This indicates that the latitude at which COLs develop at or migrate to is an important factor in their extension towards the surface.

It should be noted that the number of vertically related lows (d1COLs, 51.7% of the total COLs) found in this study is significantly more than found in the previous study by Pinheiro et al. (2020). This is likely the result of the differences in the methodology and domains used. Pinheiro et al. (2020) excludes COLs that do not develop north of 40° S or last for at least 24 h north of 40°S. An analysis of our dCOL dataset that excludes COLs with the criteria used by Pinheiro et al. (2020) reveals that a further 23% of dCOLs would be excluded from the dCOL database using these criteria. This results in the detection of fewer d1COLs (46.2% of the

**Table 1** Table of occurrence statistics of all classified COL extensions in both the Southern hemisphere and Southern African region

	dCOLs (percentage of total COLs)	sCOLs (percentage of total COLs)	d1COLs (percentage of dCOLs)	d2COLs (percentage of dCOLs)	d1aCOLs (percentage of d1COLs)	d1bCOLs (percentage of d1COLs)
S. Hemisphere (%)	57.8	31.6	89.5	10.5	53.1	46.9
S. Africa (%)	49.0	38.3	89.2	10.1	57.4	42.6
Australia–NZ (%)	63.6	26.1	89.1	10.9	52.3	47.7
S. America (%)	55.2	35.2	90.2	9.8	51.5	48.5

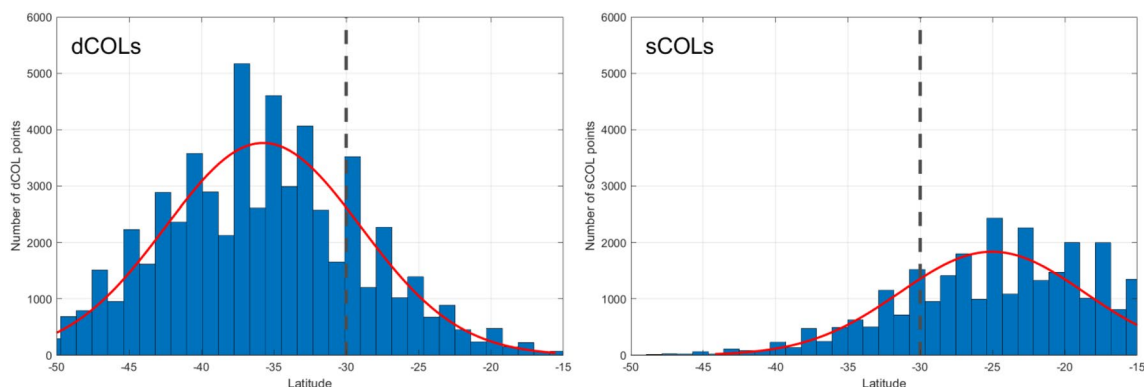


**Fig. 3** Distribution of all COL points for dCOLs (left) and sCOLs (right) with respect to latitude. Normal distribution curves are also shown by red lines. For ease of reference, the 30° S latitude is highlighted by a grey dashed line

total COLs). Additionally, Pinheiro et al. (2020) uses a relative vorticity local minimum detection algorithm to identify cyclones at all levels below the COL. This likely results in identifying closed cyclones or more defined cyclonic circulation compared to the low-pressure minima approach used in this study. The low-pressure minima approach identifies extensions with weaker troughs at some levels, increasing the number of detected COL extensions to surface cyclones. This is an appropriate methodology for this study since we aim to identify all COL extensions, whether weakly or strongly vertically coupled.

### 3.1.3 Seasonal variability of extended COLs

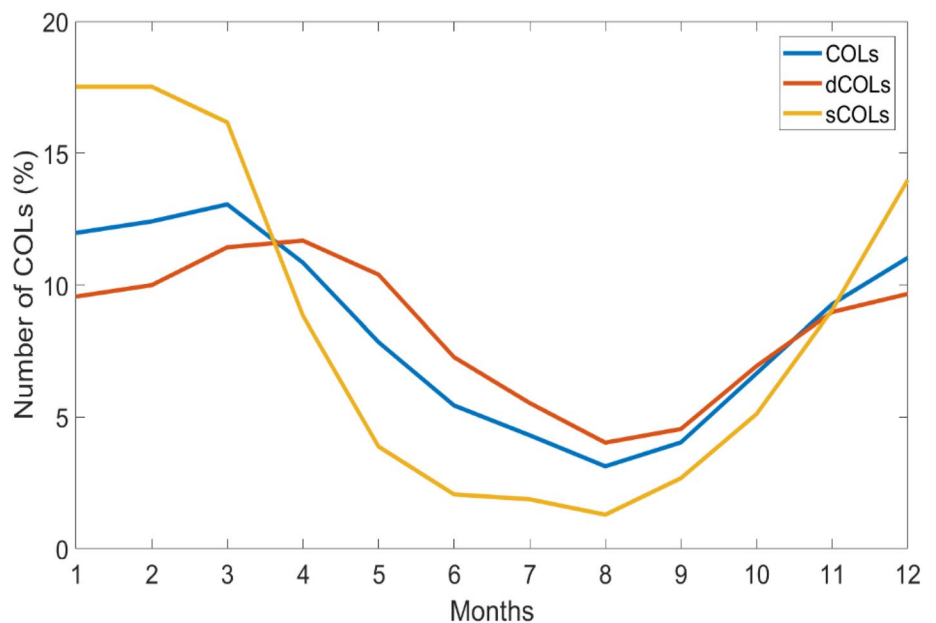
An important factor to assess in any climatology is the seasonal variability. Seasonal variability has been addressed in previous COL climatologies (Fuenzalida et al. 2005; Reboita et al. 2010; Pinheiro et al. 2017). COLs are subdivided into seasons. The season of the COL is determined by the date on which the COL is initially detected. For example, a COL with a 4-day duration detected on 31 May 2017 will be included as a May or autumn COL even though the COL persisted into June 2017. A monthly analysis is performed, and the results are shown in Fig. 4. The data shows that the COLs at 250 hPa in the database are most prevalent in the summer and autumn months with a peak in the month of March. The frequency of COLs drops throughout winter with a minimum occurrence in August. This is a very similar trend observed in previous studies of climatologies of COLs on a similar pressure level (Pinheiro et al. 2017). dCOLs seem to approximately follow the trend of the overall COL climatology. The number of dCOLs does however peak slightly later in the year, with a peak percentage of COLs

**Table 2** Seasonality of COLs in sectors of the Southern hemisphere

	COLs (%)	dCOLs (%)	sCOLs (%)
Southern Hemisphere			
Summer	<b>35.4</b>	29.2	<b>49</b>
Autumn	31.7	<b>33.5</b>	28.9
Winter	12.9	16.8	5.2
Spring	20	20.5	16.8
Southern Africa			
Summer	29.1	23.6	<b>40.4</b>
Autumn	<b>30.7</b>	<b>33.5</b>	27.4
Winter	14.6	18.4	8.4
Spring	25.6	24.4	23.7
Australia–New Zealand			
Summer	39.0	<b>33.8</b>	<b>53.1</b>
Autumn	<b>32.8</b>	<b>33.8</b>	30.6
Winter	10.4	13.4	2.4
Spring	17.8	19.0	13.8
South America			
Summer	<b>35</b>	25.3	<b>50.7</b>
Autumn	30.6	<b>32.9</b>	27.8
Winter	14.8	20.9	5.8
Spring	19.6	21	15.7

found to be in April. A definite autumnal peak can be seen in the dCOL curve in Fig. 4. Table 2 shows that 33.5% of the dCOLs occur in the autumn. This is not the case for sCOLs. sCOLs most often occur during the summer months with a definite peak in January and February. In fact, close to half (49%) of the sCOLs are found in the summer months. A sharp drop in the frequency occurs during autumn with very few sCOLs observed in the winter months. Only 5.2%

**Fig. 4** Seasonality of COLs, dCOLs and sCOLs. The percentage of each category that occur in each month are shown



of all the detected sCOLs are observed during the months of June, July and August.

Table 2 shows the inter-seasonal variability of COLs, dCOLs and sCOLs for the southern African, Australia–New Zealand and South American sectors. The seasonal trend of COLs, dCOLs and sCOLs in each sector remains relatively consistent with the overall seasonal distribution of COLs throughout the Southern Hemisphere. Both COLs and dCOLs peak towards the late summer and autumn months. sCOLs are most prevalent in the summer months with very few sCOLs present during winter. The South American sector tends to be less variable in terms of dCOLs throughout the seasons than the other sectors. This sector does have the autumnal maximum frequency as in the other two sectors, but the remaining months remain fairly consistent in terms of dCOL frequency. Another small deviation can be seen in the sCOL seasonal distribution in the southern African sector. Although the sector has a large summer maximum like all other sectors, the summer months contain 10% less sCOLs than the other sectors. Additionally, the southern African sector has a greater number of springtime sCOLs compared to the other sectors and is also the most prone sector to wintertime sCOLs.

### 3.1.4 Variability of extended COL lifetime

The lifetime of COLs has been well studied by various authors in the Southern Hemisphere (Fuenzalida et al. 2005; Reboita et al. 2010; Pinheiro et al. 2017). These systems are well known to last only a few days. The effect that COL depth has on the temporal variability of these systems is investigated here and the results shown in Fig. 5. It should

be noted that in this study, COLs are defined to last at least one day (four six-hourly timesteps). The lifespan distribution of COLs in the Southern Hemisphere as well as the sectors is very similar to what has been observed in various other studies, with the number of COLs lasting more than a day decreasing exponentially. Very few COLs are observed to occur longer than 7 days, although it does infrequently occur. Figure 5 shows that dCOLs tend to last longer than sCOLs. Close to half of the sCOLs observed have a lifetime of between 1 and 2 days in the Southern Hemisphere. Comparatively, only roughly a third of the dCOLs lasted between 1 and 2 days. For COLs observed to last longer than 2 days, there are a consistently higher frequency of dCOLs compared to sCOLs throughout all sectors of the Southern Hemisphere until at least 7 days. This is evidence that the depth of COLs could play some role in extending the lifespan of COLs. Results in each of the southern African, Australia–New Zealand and South American sectors are consistent with the temporal distribution of the Southern Hemisphere with respect to COL depth.

### 3.1.5 Mobility of extended COLs

The mobility of COLs has been analysed in previous COL climatologies using various different methodologies. Some studies (e.g., Fuenzalida et al. 2005; Reboita et al. 2010) have used the distance and time between the start and end points of each COL to determine the velocity whilst others (e.g., Pinheiro et al. 2017) calculate the zonal mean velocity of COLs. The methodologies of Reboita et al. (2010) and Fuenzalida et al. (2005) do not take into account that COLs may not move in a straight line. In this study, we update this

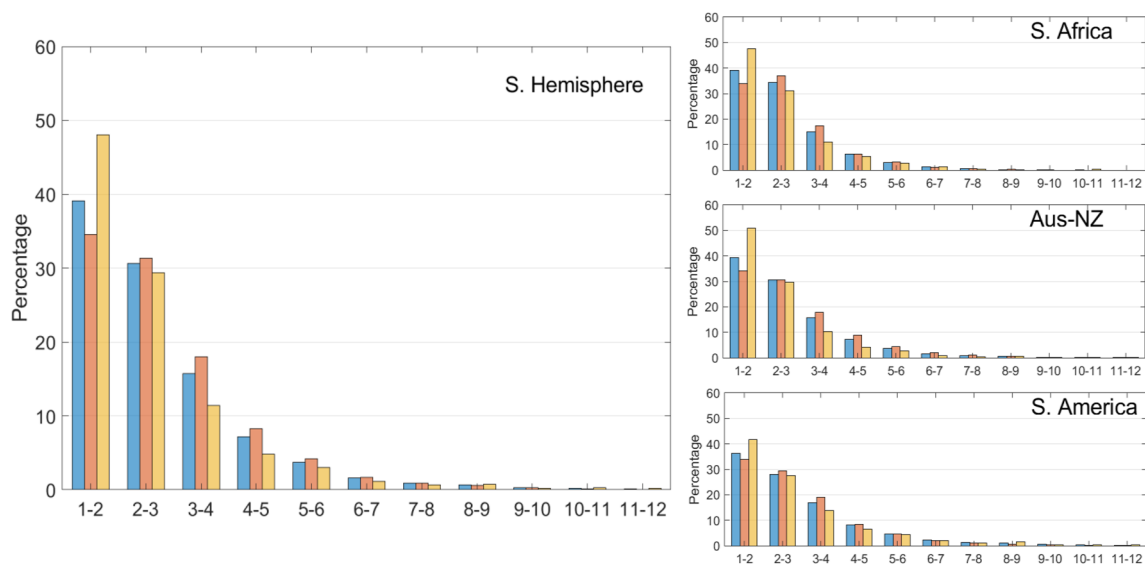


**Fig. 5** Temporal variability of COLs. The frequency distribution of the lifespan (in days) is given for COLs (blue), dCOLs (red) and sCOLs (yellow). A breakdown for the southern African, Australia–New Zealand and South American sectors are also given (right panel)

methodology by calculating the distance between each of the COL points in each COL trajectory to calculate the total distance that the COL has travelled. This provides a more accurate mean velocity for each COL.

Figure 6 shows the distribution of mean speeds for COLs, dCOLs and sCOLs. The maximum frequency of COL mean speeds is between 9 and 12 m/s. This is considerably higher than in previous studies (e.g., Reboita et al. 2010). This discrepancy however is due to the methodology used, as in this study we use a more integrated distance (which increases the distance travelled), whilst previous studies use the straight-line distance approach. There is a slight shift in the maximum mean COL velocity between sCOLs and dCOLs. dCOLs (with a maximum frequency in the 9–12 m/s category) tend to be slightly faster than sCOLs (with a maximum frequency in the 6–9 m/s category). COL mobility is relatively consistent across the three regions with very little variability in the COL mean velocity distribution as can be seen in Fig. 6.

### 3.2 RWB events and extended COLs

RWB is a known mechanism for inducing stratospheric-tropospheric exchange which may result in COL development (Ndarana and Waugh 2010). As the mechanism that drives the development of COLs, it is important to investigate whether RWB is linked to vertical extension of COLs. COLs have been climatologically linked to RWB in the Southern Hemisphere in the study by Ndarana and Waugh (2010). However, this study used NCEP/NCAR reanalysis

data whereas we make use of ERA-Interim reanalysis. As explained in Sect. 3.1, COL detection between various versions of ERA and NCEP/NCAR differs significantly as to the number of COLs detected. For example, Reboita et al. (2010) detected 50–75% more COLs using ERA-40 compared to NCEP/NCAR reanalysis data. Due to the large discrepancies between the two reanalysis datasets with respect to COL detection, it is important to confirm that the relationship between COLs and RWB events still hold using the ERA-Interim dataset. A search polygon was created for each COL. The search polygon comprised an area 60° to the west, 10° to the east and 15° north and south of each COLs initial point. RWB occurring during the life of each COL as well as up to 4 days prior to the COLs initial development are considered. If a RWB polygon in the database intersected with the search polygon, the RWB event is said to be associated with the COL. Using this methodology, 99.3% of the COLs in the database throughout the Southern Hemisphere are collocated with at least one RWB event. Together with the work by Ndarana and Waugh (2010), this reaffirms the climatological link between RWB and COLs.

The COL depth database allows for the exploration of RWB events and their link to the vertical structure of COLs. For the purposes of this study, we define a deep RWB event as an event which occurs on multiple isentropic levels simultaneously. The greater number of levels these events occur on, the deeper the event is said to be. Conversely, shallow RWB occur on fewer of these levels simultaneously. A total of four different isentropic levels (315-, 320-, 330- and 350-K) are used in this study. Therefore, the RWB depth is

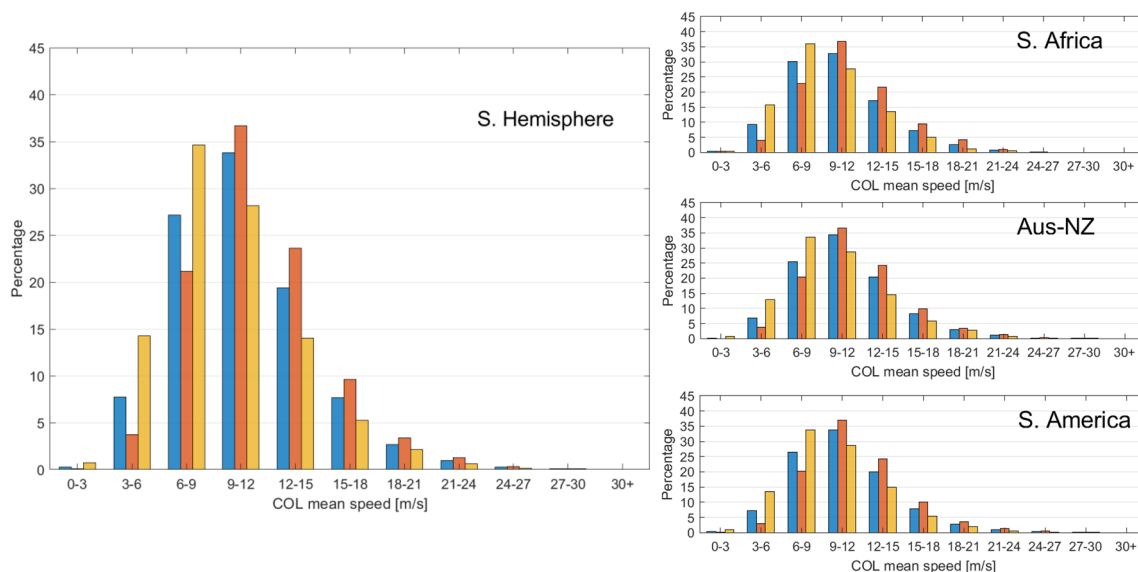


**Fig. 6** Mobility of extended COLs. The frequency distribution of the mean speed across the entire trajectory of each COL (in m/s) is given for COLs (blue), dCOLs (red) and sCOLs (yellow). A breakdown for

the southern African, Australia–New Zealand and South American sectors are also given (right panel)

ranked from 0 to 4 where 0 indicates COLs that are associated no RWB event up to 4, which indicates that a COL is affected by RWB events on all four isentropic levels. The RWB depth is calculated for both dCOLs and sCOLs and the results are shown in Fig. 7. This can also be seen visually in Fig. 8 by the composite mean geopotential height and isentropic PV contours of the initial timestep of each dCOL and sCOL. Although a rudimentary approach, the results reveal a very distinct difference in RWB depth between dCOLs and sCOLs. dCOLs are more often associated with RWB events identified on multiple isentropic levels and therefore greater RWB depths than sCOLs. About 90% of all dCOLs were

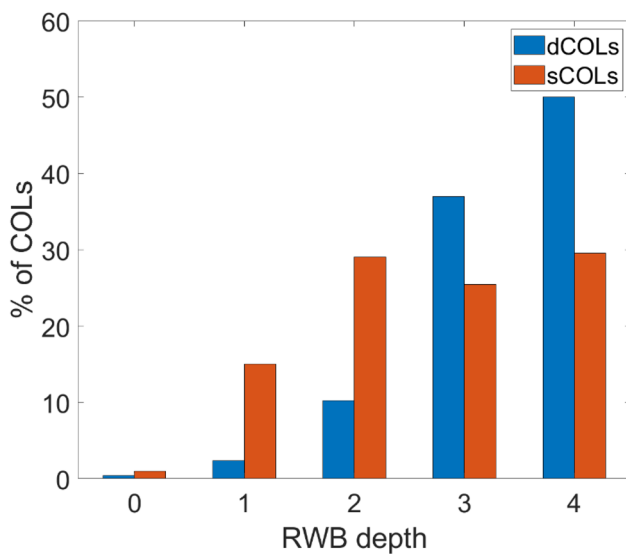


**Fig. 7** Percentage of dCOLs and sCOLs as a function of RWB depth. RWB depth is defined as the number of isentropic levels (from 315, 320, 330 and 350 K) in which an overturned  $-1.5$ ,  $-2$  or  $-2.5$  PVU contour is found

associated with RWB depths of 3 or more. sCOLs are shown to be associated with a variety of RWB depths.

RWB depth is also expressed by the dCOL and sCOL composites in Fig. 8. Multiple PV contours on multiple levels are shown to be overturning or already cut-off by the time of the first detected dCOL point. In fact, only the 350 K isentropic contours do not overturn situated to the north of the COL. Conversely, the sCOL composite shows very few isentropic PV contours overturning or cut-off surrounding the COL. Interestingly, RWB events in the presence of sCOLs generally occurs on the 350 K surface, where dCOLs show no signal of overturning. Figures 7 and 8 show that the intensity or depth of a RWB event could have an impact on the eventual extension of a COL towards the surface, with deeper RWBs on lower isentropic surfaces generally associated with deeper vertical extension.

### 3.3 Vertical PV profiles in relation to extended COLs

The depth of stratospheric intrusions is compared to the depth of COLs to understand the effect that the depth of an intrusion has on the extension of COLs. First, the stratosphere is mapped and labelled according to the algorithm by Škerlak et al. (2014) as mentioned in Sect. 2.6. The lowest level on which stratospheric PV (Label 2, in the algorithm) is then found. The stratospheric intrusion depth related to a COL is determined to be the lowest stratospheric PV value within a  $10^\circ \times 10^\circ$  grid box of the COL point. The lowest intrusion value is recorded and associated with each COL in the database. The results of the PV depth analysis are shown in Fig. 9. Stratospheric intrusion depths are calculated for both dCOLs (Fig. 9-A1) and sCOLs (Fig. 9-B1). The data shows that dCOLs are generally associated with stratospheric intrusions of the  $-1.5$  PVU contour to a depth of at least 300 hPa. sCOLs on the other hand are generally associated with  $-1.5$  PVU stratospheric intrusions of above

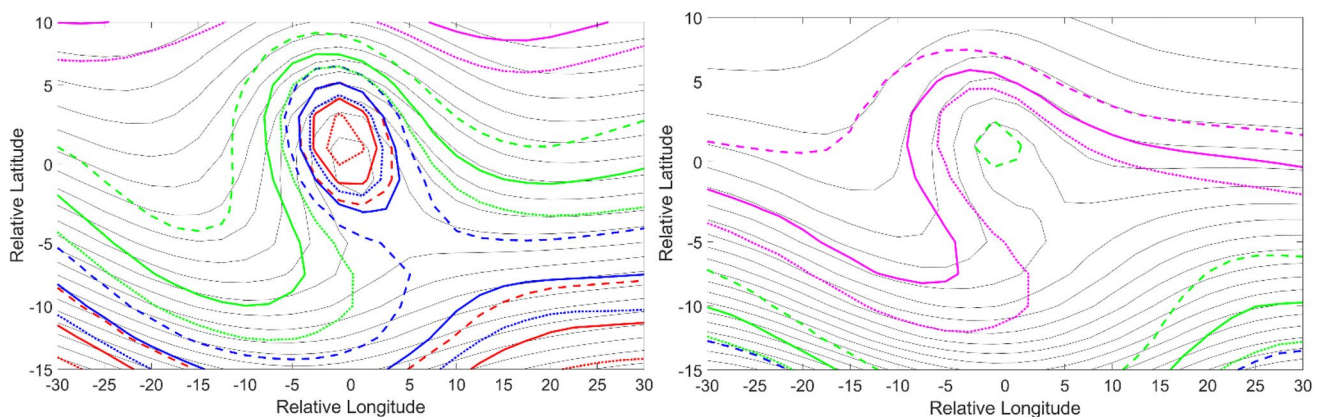


**Fig. 8** COL and isentropic PV composites for dCOLs (left) and sCOLs (right). The  $-1.5$  (dotted),  $-2$  (solid) and  $-2.5$  (dashed) PVU contours on the 315 K (red), 320 K (blue), 330 K (green) and 350 K (magenta) are shown

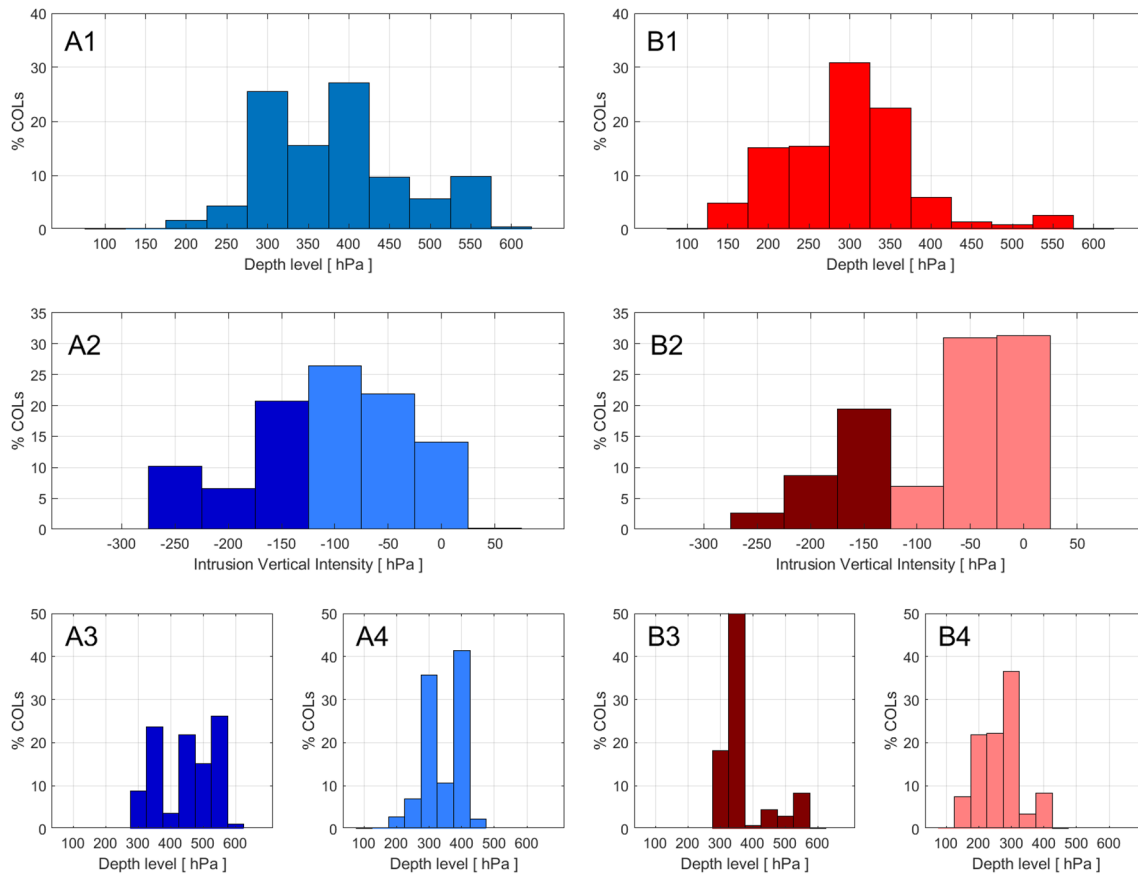


**Fig. 9** **A1** Percentage of stratospheric intrusion depths for all dCOLs. **B1** Same as for **A1** but for sCOLs. **A2** Percentage of stratospheric intrusion vertical intensities (vertical size of the stratospheric intrusion below the climatological tropopause) for all dCOLs. For ease of reference, large vertical intensities are highlighted in dark colours whilst small vertical intensities are highlighted in lighter colours. **B2**

Same as for **B1** but for sCOLs. **A3** Percentage of stratospheric intrusion depths for dCOLs with large stratospheric intrusion vertical intensity (less than or equal to  $-150$  hPa). **B3** Same as for **A3** but for sCOLs. **A4** Percentage of stratospheric intrusion depths for dCOLs with small stratospheric intrusion vertical intensity (greater than or equal to  $-100$  hPa). **B4** Same as for **A4** but for sCOLs

350 hPa. This is clear evidence that COLs that are associated with surface lows (dCOLs) are generally associated with stratospheric intrusions that are present closer to the surface. Interestingly, there exists a “middle-world” for the depth of  $-1.5$  PVU stratospheric intrusions between the 300 hPa and 350 hPa levels in which both sCOLs and dCOLs are both prevalent. Since 300–350 hPa depth intrusions are shown to be frequently associated with both sCOLs and dCOLs, it could indicate that there are other processes or mechanisms in the atmosphere which either drive surface cyclonic development or inhibit it beneath these specific COLs.

As mentioned in Sect. 3.1, dCOLs are generally found in the higher latitudes whilst sCOLs are more often found closer to the tropics. The tropopause is climatologically higher in the tropics and sub-tropics compared to the extratropics. Naturally this begs the question as to whether the vertical size or intensity of the stratospheric intrusion effects the extension of a COL to the surface or if this is related to the actual depth (or proximity to the surface) that the

intrusion reaches. To investigate this, we derive a stratospheric intrusion vertical intensity value for each of the stratospheric intrusions associated with each COL. For the purposes of this study, the stratospheric intrusion vertical intensity is defined as the stratospheric intrusion depth subtracted from the climatological mean dynamical tropopause level. The climatological dynamical tropopause height is calculated based on the average value of PV. The climatological mean PV field is compared to each COL’s stratospheric intrusion depth to find the depth of the intrusion relative to the dynamical tropopause. Figure 9 shows the results of the stratospheric intrusion vertical intensity analysis for dCOLs (Fig. 9-A2) and sCOLs (Fig. 9-B2). In this study, a large vertical intensity is regarded as a stratospheric intrusion is 150 hPa below the climatological dynamical tropopause or lower (highlighted in Fig. 9 by darker colours) whilst small vertical intensities are considered to be smaller than 150 hPa (highlighted in Fig. 9 by lighter colours). Figure 9-A2 and B2 show that sCOLs are generally associated with intrusions

with a smaller vertical extent than dCOLs. Interestingly however, dCOLs can however be associated with intrusions with smaller vertical extent whilst conversely sCOLs can be associated with intrusions with large vertical extent or intensity.

To investigate the vertical intensity of intrusions with respect to the depth they reach, we separate dCOLs and sCOLs by their vertical intensity or extent and analyse the depths that the associated stratospheric intrusions reach. The analyses are shown in Fig. 9-A3, A4, B3 and B4. Larger vertical intrusions associated with dCOLs (Fig. 9-A3) are shown to extend further to lower levels extending to at least the so-called intrusion “middle-world” (300–350 hPa). Smaller vertical intrusions associated with dCOLs are also shown to extend largely to the “middle-world” levels (Fig. 9-A4). Conversely, large vertical intensity intrusions that result in sCOL development generally largely do not extend to lower levels, only extending to the 300–350 hPa (or middle-world) levels (Fig. 9-B3). This indicates that sCOLs can be associated with vertically larger intrusions of stratospheric air. However, the fact that these intrusions do not extend towards the mid-troposphere results in the COL not extending all the way to the surface. This indicates that the depth that the intrusion reaches (proximity to the surface) is likely more important to COL extension than the vertical intensity or size of the intrusion itself.

These findings also help to explain the latitudinal and seasonal variability of COL extensions. sCOLs are more often found in the lower latitudes. The dynamical tropopause is situated climatologically further away from the surface in the lower latitudes (Kunz et al. 2011). This means that intrusions need to extend further down from the stratosphere to reach a level in which the system is prone to cyclonic development at the surface (as seen in Fig. 9-A3 and A4). The converse is true for the higher latitudes where the lower dynamical tropopause requires only small intrusions to reach a conducive level (as seen in Fig. 9-B3 and B4). A similar argument can be made for the seasonal variation of dCOLs and sCOLs. During the summer months the ITCZ moves southwards, raising the dynamical tropopause (Kunz et al. 2011) making it less likely for intrusions to reach a conducive level. This could explain the large amount of sCOL development during the summer months. With the dynamical tropopause lower in the winter months, more dCOLs are prevalent in the winter months compared to sCOLs as shown in Fig. 4.

### 3.4 Low level anomalies as extension inhibitors

The results throughout the study show that upper level processes are integral in surface cyclogenesis. These upper level processes are however coupled with low level processes which can also play a role in the development of low-pressure systems. PV theory tells us that upper level PV

anomalies also result in mirrored cyclonic motion at the surface (Hoskins et al. 1985). As a result of the north–south surface temperature gradient, the cyclonic motion at the surface will result in warm air temperature advection at the surface ahead of the upper level PV structure. Surface potential temperature ( $\theta$ ) anomalies can act like PV anomalies (Bretherton 1966). Warm (cold) surface  $\theta$  anomalies are associated with cyclonic (anticyclonic) flow around them at the surface. Both the low-level  $\theta$  and upper level PV anomalies feed off one another resulting in either their mutual amplification or decay. For the surface anomaly to be beneficial to the upper level anomaly and development of both cyclones, the system should be baroclinic such that the positive  $\theta$  anomaly lies to the east relative to the cut-off low and associated upper level PV anomaly. A surface anomaly that is out of phase with the upper level processes could be a factor that results in sCOLs with stratospheric intrusions into the intrusion “middle-world” and deeper intrusions not extending to the surface. To investigate this, we analyse  $\theta$  anomaly fields at the 1000 hPa level around each COL.  $\theta$  anomalies are calculated using mean  $\theta$  fields. We first perform a composite analysis of mean surface  $\theta$  anomalies. Composites are created at the initial detected position of each COL. The evolution of the surface PV anomalies are shown by showing composites for 3 days prior to and 3 days after the initially detected COL point of each COL. The results of this analysis for both dCOLs and sCOLs are shown in Fig. 10. The composite of dCOLs clearly shows a warm potential temperature anomaly in phase lying to the east of the COL. This warm anomaly strengthens as the COL develops and weakens once the COL begins to decay after day 1. A stark contrast is seen in the composite surface  $\theta$  anomaly for sCOLs. An extremely warm anomaly is present to the west and out of phase with the sCOL and upper level PV anomaly. Figure 10 shows that the warm  $\theta$  anomaly does not strengthen but does move closer to the COL when it develops, through maturity and decay. The warm anomaly to the west of the COL means that cyclogenesis is out of phase with the upper level processes. As a result, the intense warm  $\theta$  anomaly to the west of the COL could be an inhibitor to surface cyclonic development.

It is however notable that the entire  $\theta$  anomaly field for sCOLs is anomalously warm. Therefore, even though there is a large warm  $\theta$  anomaly out of phase with the COL, the general warm anomaly to the east of the COL axis needs further investigation. An analysis of surface 1000 hPa gph fields reveal that the surface field underneath the sCOL is under the influence of a zone of high pressure, advecting warmer tropical air to the west of the COL axis. This explains the large warm  $\theta$  anomaly as shown in Fig. 10 (right panels). An analysis of all the central pressures of all sCOL-associated surface high-pressure cells reveals that the center of the high-pressure cell can however often be located to the east of the COL axis. A composite of all of

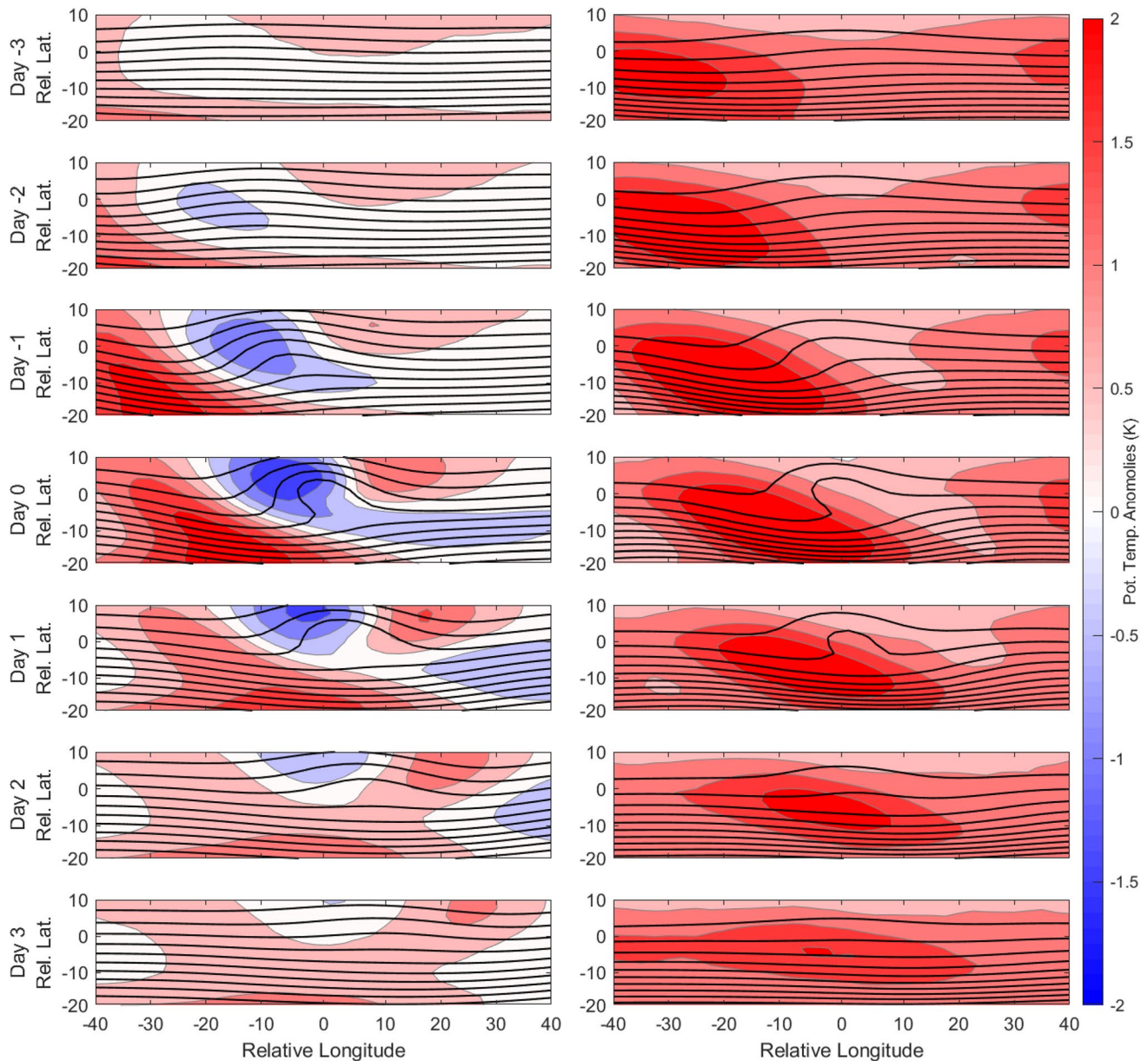


**Fig. 10** Composite analysis of mean 1000 hPa potential temperature anomalies relative to the position of the COLs initial detected position. Composites for dCOLs (left) and sCOLs (right) are shown for

3 days prior and 3 days after the COLs initial detection. Relative latitudes and longitudes are relative to the initial position of the detected COL

the eastward-located shows that this surface high extends westwards beneath the COL axis. The anticyclonic flow results in flow from the warmer tropics on both sides of the COL axis and a more intense warm anomaly to the east of the COL axis. As this situation happens frequently, this explains the small warm  $\theta$  anomaly signals shown to the east of the COL axis in Fig. 10. Although these anomalies

could induce cyclogenetic forcing in phase with the COL, the strong high-pressure zone persists long enough such that the COL does not extend to a low-pressure zone at the surface.

Another notable difference in the composite of Fig. 10 is the cold anomaly  $\theta$  lying to the west of the dCOL. Conversely, no cold  $\theta$  anomaly is seen below that of the sCOL.



As with the warm  $\theta$  anomaly of the dCOLs, the cold anomaly strengthens as the COL develops and weakens once the COL begins to decay after day 1. Cold low-level anomalies, associated with anticyclonic flow, have also been linked with RWB resulting in ridging highs over the South African region (Ndarana et al. 2018). Conversely to warm  $\theta$  anomalies, cold surface  $\theta$  anomalies are responsible for anticyclonic development. The lack of cold  $\theta$  anomaly present for sCOLs in Fig. 10 shows that dCOL extensions and deep intrusions of stratospheric air could also be critical for the development and ridging of surface highs. Ridging surface highs are an important mechanism for South African rainfall and severe weather (Ndarana et al. 2018).

We now show that the majority of the sCOLs contain a  $\theta$  anomaly that is out of phase with the upper level processes. In a  $10^\circ \times 20^\circ$  latitude-longitude  $\theta$  anomaly grid box around the initially detected position of the COL, the relative longitudinal position of the maximum value of  $\theta$  ( $\theta_{max}$ ) to the COL are recorded. Negative relative  $\theta_{max}$  longitudes indicate that the surface  $\theta$  anomaly lags behind the upper level processes and is out of phase with the COL (as seen in the composite  $\theta$  field in Fig. 10). If a COL point has a negative relative longitude  $\theta_{max}$  the COL is marked as a “unconductive surface” COL. We also consider that the  $\theta$  grid could contain multiple areas of high anomalous  $\theta$  values. Therefore, a COL is also marked as an unconductive surface COL if  $\theta_{max}$  has a positive relative longitude but a high anomalous  $\theta$  value is found with a negative relative longitude. The converse procedure reveals COL points in which the surface is conductive. In this study a high anomalous  $\theta$  value is a value that is at least 75% of the  $\theta_{max}$  value of the  $\theta$  grid.

The analysis is performed using the first detected position and the last detected position of each sCOL. This choice gives insight into the surface characteristics throughout the lifecycle of the COL as well as any shifts in surface characteristics that may occur during the lifecycle of the COL. The analysis shows that only 12.1% of the sCOLs detected have conductive surface characteristics at the first position of the COL. This rises slightly to 17.2% for the last detected position of each sCOL. The procedure is also performed for dCOLs where positive relative  $\theta_{max}$  longitudes or high  $\theta$  values with positive relative longitudes are searched for. 66.1% of dCOLs are marked as conductive surface COLs at the first detected COL position. The amount of dCOLs with conductive surface characteristics however rises to 73.9% by the end of the COLs lifecycle. The low percentage of sCOLs with conductive surface PV characteristics and the high percentage of dCOLs with conductive surface PV characteristics show the importance of the surface PV characteristics being

in phase with the upper level processes. If they are not in phase, they can be an inhibitor to COLs extending to the surface. A warm  $\theta$  anomaly in phase (as shown in Fig. 10) can also be a contributor to cyclonic surface development.

### 3.5 The evolution of COL extensions

Conceptually, we think of COL extensions developing in the upper troposphere and developing and extending towards the surface (Nieto et al. 2005). The temporal aspects of COL vertical extensions are investigated here through composites relative to a COLs initial position. In Sect. 3.1, d1COLs were classified by the relative time a surface low was detected. In this classification d1aCOLs, in which the surface low develops at (within 12 h) or after the COL are associated with COLs which develop their own surface lows. The temporal evolution of d1aCOLs are therefore studied separately to look at the COLs vertical extension. Composites of latitudinal cross-sections of PV through the initial COL point and composites of geopotential heights at various pressure levels are shown in Fig. 11. PV cross-sectional composites of d1aCOLs (top panels of Fig. 11) show that the dynamical tropopause begins to extend towards the surface roughly 2 days before the upper closed low pressure forms. The stratospheric intrusion grows over the next 48 h to form a tower of increased PV through to the low levels. This is likely a result of the variability of stratospheric intrusion depths that result that can link with low-level diabatic heating PV anomalies.

Geopotential height fields throughout the troposphere reveal that as the PV intrusion extends towards the surface, cyclogenesis starts to occur throughout the troposphere simultaneously. This contradicts our conceptual model of COL extensions whereby the upper level low develops first with subsequent extension and development towards the surface. The composite indicates that a closed surface cyclone develops at the same time as the COL. This suggests that the surface cyclone and each d1aCOL generally develop quasi-simultaneously. An analysis of the time of the first detected surface cyclone compared to the time of the first detected d1aCOL point (as shown in Fig. 12) indicates that this is indeed the case. Almost 90% of surface cyclones developed between 12 h before and 24 h after the first detected d1aCOL point. Both the COL and the surface cyclone start to degrade after 24–48 h, with the geopotential composite returning close to the atmospheric state before the COLs development.

The evolution surface pressure system is reminiscent of the  $\theta$  anomaly evolution as shown in Fig. 10. The placement and timing of the surface cyclones development is consistent

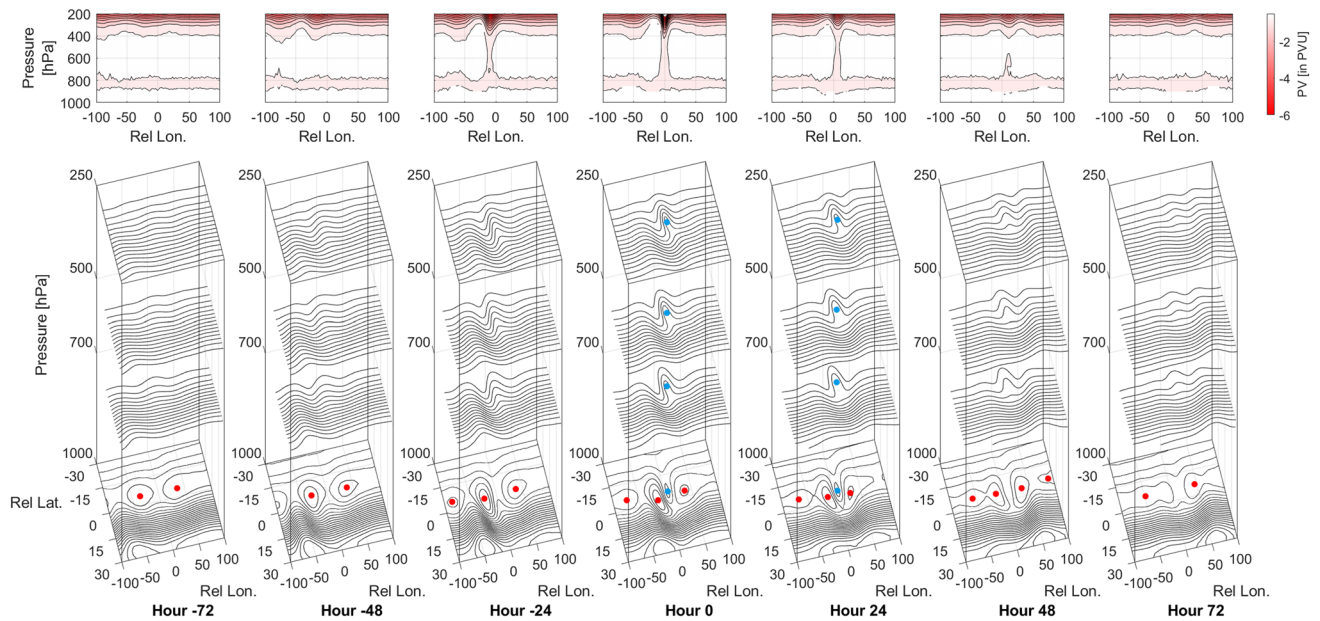


**Fig. 11** Temporal evolution by means composites of PV (top panel) and geopotential height fields (bottom panel) relative to the initial position of all d1aCOLs with a lifespan of at least 3 days. Composites are provided for between 3 days (72 h) prior to and 3 days after the initial COL position are provided. PV composites in the top panels are latitudinal cross-sections through the latitude of the first point in

each COL trajectory. Geopotential pressure composites at 250 hPa, 500 hPa, 700 hPa and 1000 hPa are given in the bottom panels to show the vertical evolution of the pressure systems during d1aCOL development. For ease of reference, relevant high-pressure regions are denoted with red dots whilst low pressure areas are denoted by blue dots

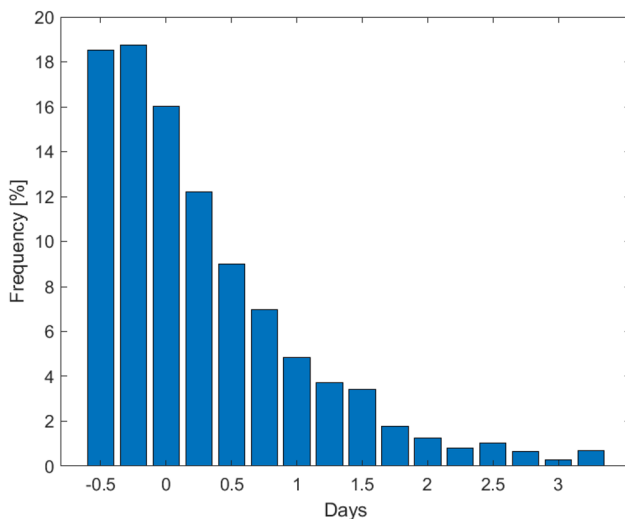


**Fig. 12** Frequency of time difference (in days) between the first detected surface low pressure and first detected point in each d1aCOL trajectory

with the development of the warm  $\theta$  anomaly. Moreover, the surface high ridging process is clearly seen on the 1000 hPa geopotential composites. The anticyclone to the west of the

surface cyclone and COL, develops and strengthens throughout the development of the COL and intrusion of the high-PV stratospheric air. This too is consistent with the development of the cold  $\theta$  anomaly in shown in Fig. 10.

d1bCOLs (dCOLs in which a closed surface cyclone develops more than 12 h before the COL) are associated with COLs that develop over already existing baroclinic zones or surface lows. The vertical evolution of d1bCOLs is also investigated by means of composite analysis in Fig. 13. The cross-sectional PV and stratospheric intrusion evolution are similar to that associated with d1aCOLs (Fig. 11). Therefore, the PV mechanisms that drive the d1bCOLs development from the upper troposphere are relatively similar to d1aCOLs. As expected, a surface trough is present beneath the COL at the surface 72 h before the COLs development. The surface trough develops into a surface cyclone 24 h before the development of the COL. A notable difference to the d1aCOL evolution, is increased amplitude of the trough throughout the troposphere at 24 and 48 h before the COL develops. The enhanced development is likely a result of the enhanced cyclonic development at the surface as this is the only factor changed between d1aCOLs and d1bCOLs. This is consistent with the theoretical concepts explored by Hoskins et al. (1985) whereby a surface cyclone

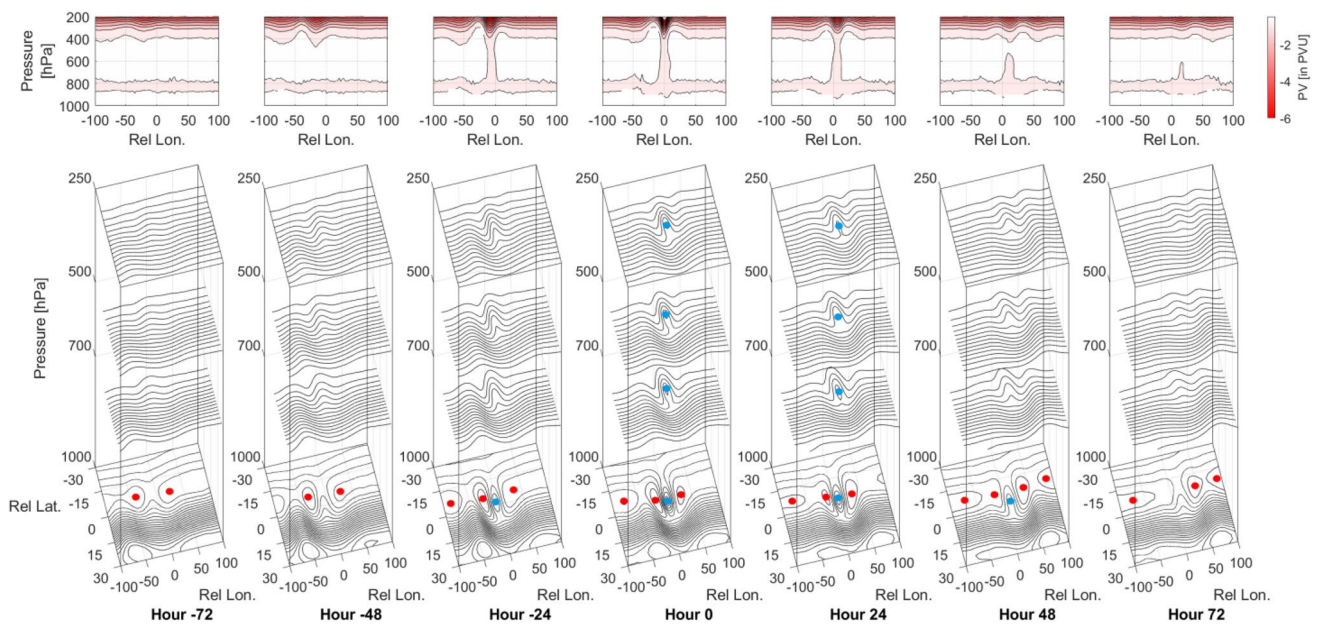


Fig. 13 Same as in Fig. 11 but for d1bCOLs

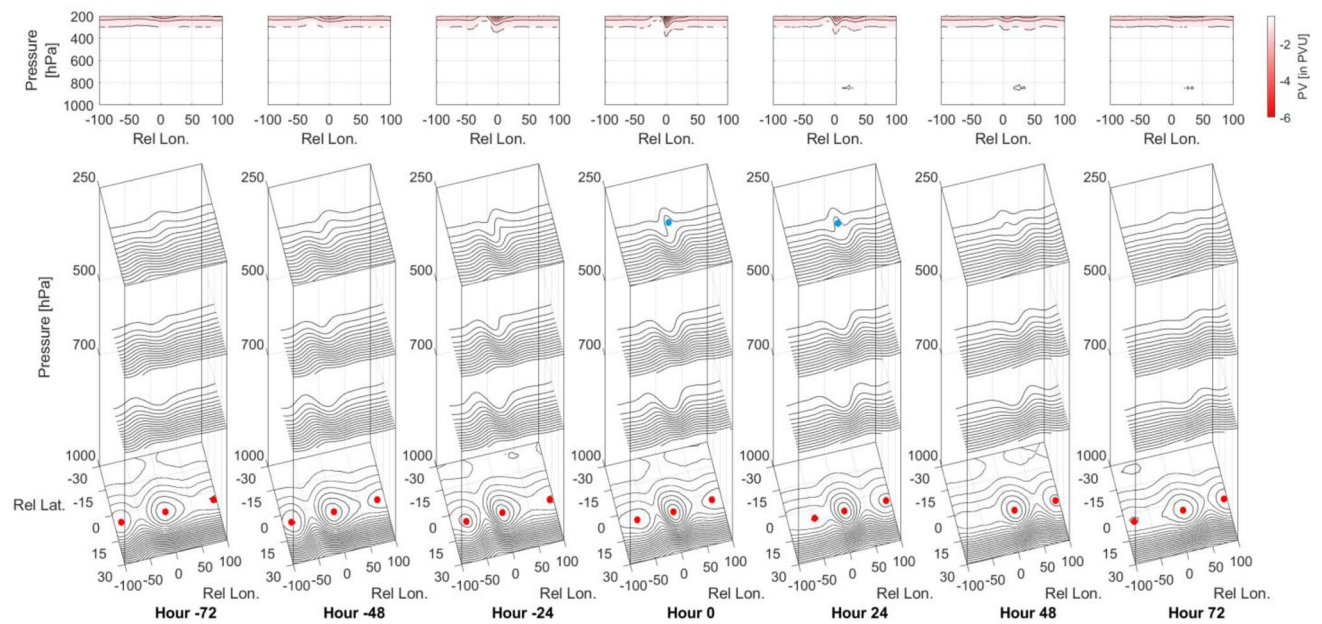


Fig. 14 Same as in Fig. 11 but for sCOLs

can be beneficial to the COLs development and visa versa if they are in phase with one another. In addition, the surface cyclone at the surface associated with the d1bCOL persists for longer than with the d1aCOL, with a closed low pressure contour still visible on the surface 2 days after the

COLs initial development. This is likely a result of the significant deepening that takes place when a COL develops over an existing surface low pressure system as explained in Sect. 3.1.1 and seen in the case study by Barnes et al. (2021) in the south Atlantic.

Finally, the vertical evolution associated with sCOLs is analysed. The composites of cross-sectional PV and geopotential heights at various levels, as with d1aCOLs and d1bCOLs, are shown in Fig. 14. The cross-sectional PV composites show significant differences to that of the d1COLs. Notably, the dynamical tropopause is situated further from the ground. This is consistent with the associated seasonal and latitudinal variability of sCOLs as previously discussed. Also notably, the PV intrusion is far shallower than that of the d1COLs composites with no enhanced PV in the low to mid-levels and is consistent with the findings shown in Fig. 9. The vertical profile of the geopotential height composites also shows large differences to that of the d1COLs in the mid- and low-levels. The 500 hPa and 700 hPa mean fields start to ridge directly beneath the developing COL. This occurs 48–72 h before the development of the COL. The mid- to low-level ridge extends to a well-developed high-pressure cell at the surface. As discussed previously, the surface flow feeds back into the circulation above it including the that of COL. Thus, the presence of the well-developed high at the surface could contribute the ridging that is seen in the mid- to low-levels. A surface trough can also be seen to the west of the COL axis. This is coincident with the warm surface  $\theta$  anomaly zone associated with sCOLs as shown in Fig. 10. This trough is out of phase with the COL as previously discussed.

#### 4 Summary and conclusion

In this study, ERA-Interim reanalysis data is analysed to gain an understanding of the processes that result in the extension of COLs to the surface and the development of surface cyclones. To achieve this, a COL climatology is developed. COL climatologies have been extensively done throughout the Southern Hemisphere at various atmospheric levels for using various methodologies. This study detects COLs at the 250 hPa level using an exhaustive detection algorithm taking into account local geopotential minima, closed cyclonic circulation as well as a cold core condition. The resulting COL climatology is on par with other similar climatologies throughout the Southern Hemisphere. In this study we extend this climatology by calculating the vertical depth of the associated COLs and their relationship to a surface cyclone. The vertical depth analysis reveals that in the Southern Hemisphere, COLs are generally deep, with nearly 60% of all Southern Hemisphere COLs extending to the surface (1000 hPa). The

majority of the remainder of COLs are relatively shallow (up to 500 hPa).

The COL vertical extension climatology naturally leads to the classification of COLs in terms of their vertical depth and relationship to a surface cyclone. Deep COLs (dCOLs), COLs which extend vertically to the 1000 hPa level, are classified into dCOLs with defined cyclonic circulation (d1COLs) and those without (d2COLs). The majority (~90%) of these dCOLs are associated with defined cyclonic circulations. We further classify d1COLs by the timing of the detection of the closed surface low. d1aCOLs are defined as d1COLs whose surface cyclones are first detected from 12 h before the development of the COL. The remainder are classified as d1bCOLs. 53.1% of COLs are classified as d1aCOLs in the Southern Hemisphere. This reveals that COLs do not necessarily always develop closed circulations through their own dynamic development mechanisms. COLs can frequently develop in regions where closed low pressures already exist. Pre-existing surface cyclones provide a baroclinic environment and allows the COL to readily extend to the surface. Although d1bCOLs do not develop their own closed surface circulations, the upper level dynamics still influence the surface cyclones. In fact, over three quarters of the classified d1bCOLs resulted in some form of deepening of associated 1000 hPa geopotential minima during the lifecycle of the COL. As a result of this deepening, surface cyclones associated with d1bCOLs generally have a closed circulation for a longer period of time from the COLs initial development than d1aCOLs.

COL extension is also found to be spatially, seasonally, and temporally variable. dCOLs have a high frequency of occurrence in the Australia–New Zealand sector of the Southern Hemisphere. The southern African sector conversely has a relatively low frequency of dCOLs and the largest frequency of sCOLs. Almost half of the sCOLs identified developed in the summer months, with the peak in frequency in COLs and dCOLs arriving during the autumn months. During the warmer summer months, the meteorological equator shifts southwards resulting in the dynamical tropopause being situated at a higher level in the troposphere. This means that even deep – 1.5 PVU stratospheric intrusions do not extend to the mid-troposphere to stimulate surface cyclogenesis. Similar reasoning also explains the vast amount of sCOLs found in or near the subtropics. The southern African region shows the lowest frequency of sCOLs in summer but has the highest frequency of sCOLs. COL depth also seems to play a role in the lifespan of COLs. COLs generally survive for up to 4 days. dCOLs however show a tendency to live

longer than sCOLs throughout the Southern Hemisphere. The lifetime of dCOLs are likely assisted by the surface cyclone which, in phase with the upper level low, can enhance the COL's development.

The mechanisms, from a PV perspective, resulting in the vertical extension of COLs are also explored in this study. COLs are known to be associated with stratospheric intrusions of high-PV air into the troposphere. The mechanism for bringing this stratospheric air into the troposphere through the development of COLs has been linked to RWB (Ndarana and Waugh 2010). This link is re-established using ERA-Interim reanalysis showing that most COLs are associated with RWB breaking along the dynamical tropopause. A preliminary analysis undertaken in this study of RWB depth associated with differing COL vertical extension is also performed. It is shown that dCOLs are more likely to be associated with RWB events identified on multiple levels and contours compared to sCOLs. A COL composite analysis reveals that sCOLs are more likely to be associated with RWB on high isentropic levels whilst dCOLs occur on lower isentropic PV contours. This indicates that RWB depth or intensity could be a factor in producing deeper COL vertical depths.

The depth of stratospheric intrusions and their effect on COL depth is analysed by compiling a climatology of stratospheric intrusions throughout the Southern Hemisphere. This is achieved using a labelling technique defining the stratosphere as a maximum value of PV ( $-1.5$  PVU and  $-2$  PVU). The results show that dCOLs are more often associated with deeper stratospheric intrusions compared to sCOLs. There does however exist a "middle world", independent of the PV definition of the stratosphere where both dCOLs and sCOLs can frequently exist. This implies that although upper level PV processes are highly influential, processes in the lower troposphere could influence the depth that a COL reaches. This notion is investigated by means of surface  $\theta$  anomalies. Positive  $\theta$  anomalies are known to represent PV-like anomalies at the surface and induce cyclonic circulations. The majority of sCOLs detected are collocated with  $\theta$  anomalies that lag behind the COL. As the upper and lower processes are out of phase, cyclonic development is hindered throughout the troposphere. The dependence of sCOLs on surface processes reveals the importance of the dynamics of the

entire troposphere in the development of these systems. The stratospheric depth analysis also reveals that it is the final depth that is most important in the development of dCOLs rather than the relative depth of the intrusion. Intrusions are required to extend closer to the surface in order to link up with surface processes and further influence surface cyclonic motion.

The proximity of the dynamical tropopause to the surface is likely a major contributor to the development and variability of COL extensions. The dynamical tropopause is situated further from the surface during the summer months and is climatologically higher closer to the tropics. As a result, stratospheric intrusions are required to "reach" further towards the surface in order to produce surface cyclones in summer and in the subtropics. It has been found that even though sCOLs can be associated with vertically larger intrusions of high-PV air, the stratospheric air does not extend very close to the surface as a result of the higher dynamical tropopause height in the summer and sub-tropical latitudes. dCOLs peak in frequency later in autumn (April) than sCOLs (January–February) and the total COLs (March) as the dynamical tropopause is still too high for vertically larger stratospheric intrusions to have an effect on surface cyclogenesis. Composite PV cross sections also show that sCOLs are generally associated with dynamical tropopauses which are further from the surface than dCOLs.

Importantly, a composite analysis of geopotential heights under d1aCOLs shows that the COLs extension is not a slow, extension towards the surface. A trough amplifies throughout the troposphere while the COL develops. The surface cyclone generally becomes closed within a day of when the COL is visible in the upper levels. COL extensions are also associated with ridging at the surface behind the passage of the COL and surface cyclone. This process is also visible in cold surface  $\theta$  anomalies that lag behind the passage of the dCOL.

## Appendix: COL detection algorithm schematics

See Fig. 15.

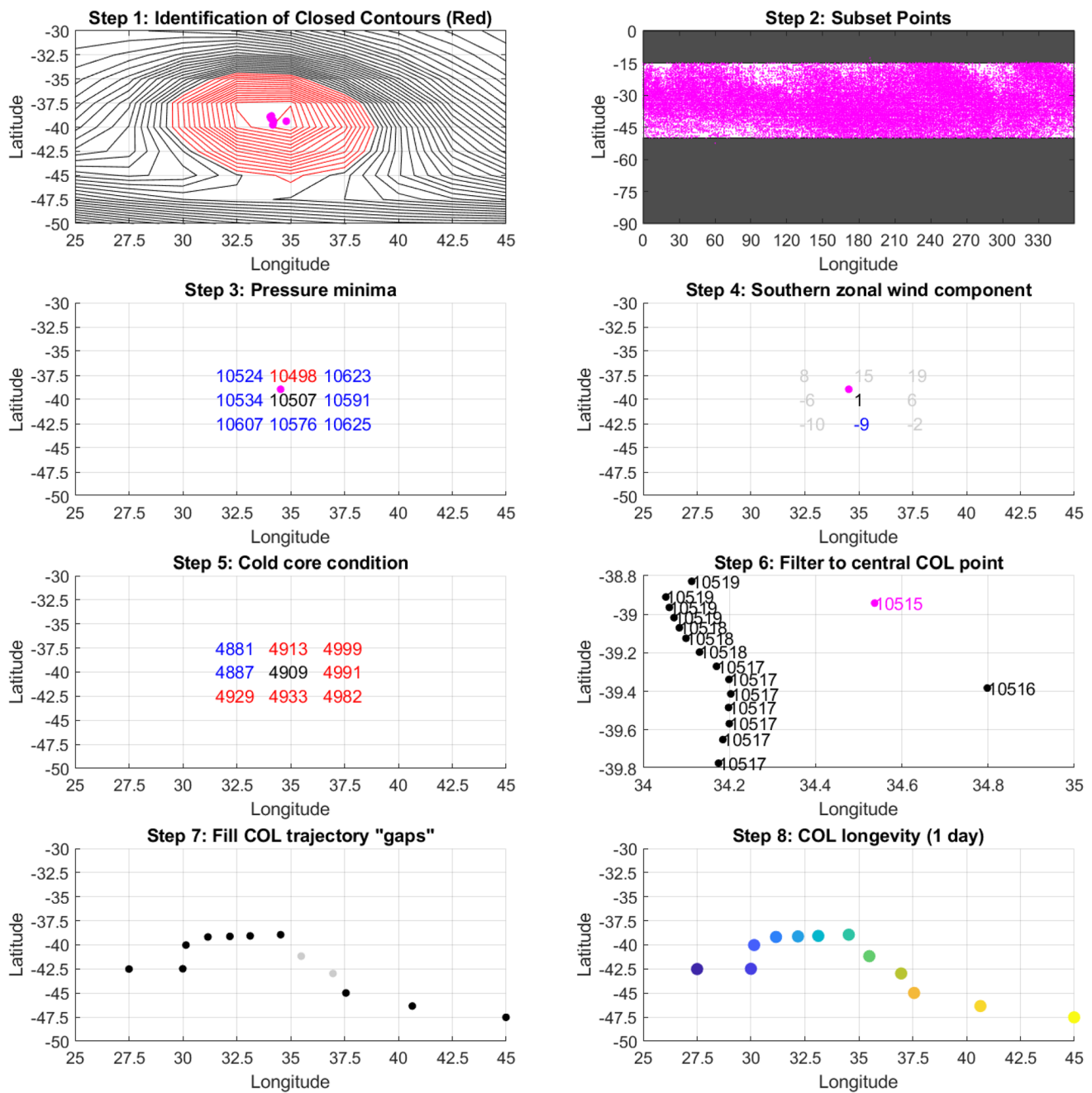


**Fig. 15** A schematic of the COL detection algorithm as described in Sect. 2.2

**Author contributions** MAB, under the supervision, review, and guidance of both TN and WAL, conceived of all the ideas in this manuscript. MAB performed all the analysis for this work and wrote the manuscript. The authors would also like to thank the three anonymous reviewers whose contributions and suggestions added significantly to this work.

## References

- Baray JL, Baldy S, Diab RD, Cammas JP (2003) Dynamical study of a tropical cut-off low over South Africa, and its impact on tropospheric ozone. *Atmos Environ* 37:1475–1488. [https://doi.org/10.1016/S1352-2310\(02\)00999-8](https://doi.org/10.1016/S1352-2310(02)00999-8)
- Barnes EA, Hartmann DL (2012) Detection of Rossby wave breaking and its response to shifts of the midlatitude jet with

- climate change. *J Geophys Res Atmos* 117:1–17. <https://doi.org/10.1029/2012JD017469>
- Barnes MA, Turner K, Ndarana T, Landman WA (2021) Cape storm: a dynamical study of a cut-off low and its impact on South Africa. *Atmos Res* 249:105290. <https://doi.org/10.1016/j.atmosres.2020.105290>
- Bell GD, Bosart LF (1993) A case study diagnosis of the formation of an upper-level cutoff cyclonic circulation over the Eastern United States. *Mon Weather Rev* 121:1635–1655. [https://doi.org/10.1175/1520-0493\(1993\)121%3c1635:ACSDO%3e2.0.CO;2](https://doi.org/10.1175/1520-0493(1993)121%3c1635:ACSDO%3e2.0.CO;2)
- Bretherton FP (1966) Critical layer instability in baroclinic flows. *Q J R Meteorol Soc* 92:325–334. <https://doi.org/10.1002/qj.49709239302>
- Čampa J, Wernli H (2012) A PV perspective on the vertical structure of mature midlatitude cyclones in the Northern Hemisphere. *J Atmos Sci* 69:725–740. <https://doi.org/10.1175/JAS-D-11-050.1>
- Campetella CM, Possia NE (2007) Upper-level cut-off lows in southern South America. *Meteorol Atmos Phys* 96:181–191. <https://doi.org/10.1007/s00703-006-0227-2>
- Dee DP, Uppala SM, Simmons AJ et al (2011) The ERA-Interim reanalysis: configuration and performance of the data assimilation system. *Q J R Meteorol Soc* 137:553–597. <https://doi.org/10.1002/qj.828>
- Engelbrecht CJ, Landman WA, Engelbrecht FA, Malherbe J (2015) A synoptic decomposition of rainfall over the Cape south coast of South Africa. *Clim Dyn* 44:2589–2607. <https://doi.org/10.1007/s00382-014-2230-5>
- Esler JG, Haynes PH (1999) Baroclinic wave breaking and the internal variability of the tropospheric circulation. *J Atmos Sci* 56:4014–4031. [https://doi.org/10.1175/1520-0469\(1999\)056%3c4014:BWBATI%3e2.0.CO;2](https://doi.org/10.1175/1520-0469(1999)056%3c4014:BWBATI%3e2.0.CO;2)
- Favre A, Hewitson B, Lennard C et al (2013) Cut-off lows in the South Africa region and their contribution to precipitation. *Clim Dyn* 41:2331–2351. <https://doi.org/10.1007/s00382-012-1579-6>
- Flaounas E, Raveh-Rubin S, Wernli H et al (2015) The dynamical structure of intense Mediterranean cyclones. *Clim Dyn* 44:2411–2427. <https://doi.org/10.1007/s00382-014-2330-2>
- Fuenzalida HA, Sánchez R, Garreaud RD (2005) A climatology of cutoff lows in the Southern Hemisphere. *J Geophys Res Atmos* 110:1–10. <https://doi.org/10.1029/2005JD005934>
- Funatsu BM, Gan MA, Caetano E (2004) A case study of orographic cyclogenesis over South America. *Atmosfera* 17:91–113
- Holton JR, Hakim GJ (2013) An introduction to dynamic meteorology. Elsevier, Amsterdam
- Hoskins BJ, McIntyre ME, Robertson AW (1985) On the use and significance of isentropic potential vorticity maps. *Q J R Meteorol Soc* 111:877–946. <https://doi.org/10.1002/qj.49711147002>
- Hsieh Y-P (1949) An investigation of a selected cold vortex over North America. *J Meteorol* 6:401–410. [https://doi.org/10.1175/1520-0469\(1949\)006%3c0401:AIOASC%3e2.0.CO;2](https://doi.org/10.1175/1520-0469(1949)006%3c0401:AIOASC%3e2.0.CO;2)
- Iwabe CMN, Da Rocha RP (2009) An event of stratospheric air intrusion and its associated secondary surface cyclogenesis over the South Atlantic Ocean. *J Geophys Res Atmos* 114:1–15. <https://doi.org/10.1029/2008JD011119>
- Kalnay E, Kanamitsu M, Kistler R et al (1996) The NCEP/NCAR 40-year reanalysis project. *Bull Am Meteorol Soc* 77:437–471. [https://doi.org/10.1175/1520-0477\(1996\)077%3c0437:TNYRP%3e2.0.CO;2](https://doi.org/10.1175/1520-0477(1996)077%3c0437:TNYRP%3e2.0.CO;2)
- Kleinschmidt E (1950) Über Aufbau und Entstehung von Zyklonen. *Meteorol Rdsch* 3:1–6
- Kunz A, Konopka P, Müller R, Pan LL (2011) Dynamical tropopause based on isentropic potential vorticity gradients. *J Geophys Res* 116:D01110. <https://doi.org/10.1029/2010JD014343>
- Lackmann GM (2011) Midlatitude synoptic meteorology: dynamics, analysis and forecasting. American Meteorological Society, Boston
- Liberato MLR (2014) The 19 January 2013 windstorm over the North Atlantic: large-scale dynamics and impacts on Iberia. *Weather Clim Extrem* 5:16–28. <https://doi.org/10.1016/j.wace.2014.06.002>
- Mcintyre ME, Palmer TN (1983) Breaking planetary waves in the stratosphere. *Nature* 305:593–600. <https://doi.org/10.1038/305593a0>
- Muñoz C, Schultz D, Vaughan G (2020) A midlatitude climatology and interannual variability of 200- and 500-hPa cut-off lows. *J Clim* 33:2201–2222. <https://doi.org/10.1175/JCLI-D-19-0497.1>
- Ndarana T, Waugh DW (2010) The link between cut-off lows and Rossby wave breaking in the Southern Hemisphere. *Q J R Meteorol Soc* 136:869–885. <https://doi.org/10.1002/qj.627>
- Ndarana T, Waugh DW (2011) A Climatology of Rossby Wave Breaking on the Southern Hemisphere Tropopause. *J Atmos Sci* 68:798–811. <https://doi.org/10.1175/2010JAS3460.1>
- Ndarana T, Bopape MJ, Waugh D, Dyson L (2018) The influence of the lower stratosphere on ridging Atlantic ocean anticyclones over South Africa. *J Clim* 31:6175–6187. [https://doi.org/10.1175/1520-0469\(1996\)053,3013:IOBSOT.2.0.CO;2](https://doi.org/10.1175/1520-0469(1996)053,3013:IOBSOT.2.0.CO;2)
- Nieto R, Gimeno L, de la Torre L et al (2005) Climatological features of cutoff low systems in the Northern Hemisphere. *J Clim* 18:3085–3103. <https://doi.org/10.1175/JCLI3386.1>
- Palmén E (1949) Origin and structure of high-level cyclones South of the: Maximum Westerlies. *Tellus* 1:22–31. <https://doi.org/10.1111/j.2153-3490.1949.tb01925.x>
- Palmen E, Newton C (1969) Atmospheric circulation systems. Academic Press, New York
- Pang H, Fu G (2017) Case study of potential vorticity tower in three explosive cyclones over Eastern Asia. *J Atmos Sci* 74:1445–1454. <https://doi.org/10.1175/JAS-D-15-0330.1>
- Pinheiro HR, Hodges KI, Gan MA, Ferreira NJ (2017) A new perspective of the climatological features of upper-level cut-off lows in the Southern Hemisphere. *Clim Dyn* 48:541–559. <https://doi.org/10.1007/s00382-016-3093-8>
- Pinheiro HR, Hodges KI, Gan MA (2019) Sensitivity of identifying cut-off lows in the Southern Hemisphere using multiple criteria: implications for numbers, seasonality and intensity. *Clim Dyn*. <https://doi.org/10.1007/s00382-019-04984-x>
- Pinheiro H, Gan M, Hodges K (2020) Structure and evolution of intense austral cut-off lows. *Q J R Meteorol Soc*. <https://doi.org/10.1002/qj.3900>
- Porcù F, Carrassi A, Medaglia CM et al (2007) A study on cut-off low vertical structure and precipitation in the Mediterranean region. *Meteorol Atmos Phys* 96:121–140. <https://doi.org/10.1007/s00703-006-0224-5>
- Rautenbach C, Daniels T, de Vos M, Barnes MA (2020) A coupled wave, tide and storm surge operational forecasting system for South Africa: validation and physical description. *Nat Hazards*. <https://doi.org/10.1007/s11069-020-04042-4>
- Reboita MS, Nieto R, Gimeno L et al (2010) Climatological features of cutoff low systems in the Southern Hemisphere. *J Geophys Res Atmos* 115:1–15. <https://doi.org/10.1029/2009JD013251>
- Singleton AT, Reason CJC (2007a) Variability in the characteristics of cut-off low pressure systems over subtropical southern Africa. *Int J Climatol* 27:295–310. <https://doi.org/10.1002/joc.1399>
- Singleton AT, Reason CJC (2007b) A numerical model study of an intense cutoff low pressure system over South Africa. *Mon Weather Rev* 135:1128–1150. <https://doi.org/10.1175/mwr3311.1>
- Škerlak B, Sprenger M, Wernli H (2014) A global climatology of stratosphere–troposphere exchange using the ERA-Interim data set from 1979 to 2011. *Atmos Chem Phys* 14:913–937. <https://doi.org/10.5194/acp-14-913-2014>

- Sprenger M (2003) Tropopause folds and cross-tropopause exchange: a global investigation based upon ECMWF analyses for the time period March 2000 to February 2001. *J Geophys Res* 108:8518. <https://doi.org/10.1029/2002JD002587>
- Sprenger M, Wernli H, Bourqui M (2007) Stratosphere-troposphere exchange and its relation to potential vorticity streamers and cut-offs near the extratropical tropopause. *J Atmos Sci* 64:1587–1602. <https://doi.org/10.1175/JAS3911.1>
- Uccellini LW, Keyser D, Brill KF, Wash CH (1985) The Presidents' Day cyclone of 18–19 February 1979: influence of upstream trough amplification and associated tropopause folding on rapid cyclogenesis. *Mon Weather Rev* 113:962–988
- van Delden A, Neggers R (2003) A case study of tropopause cyclogenesis. *Meteorol Appl* 10:187–199. <https://doi.org/10.1017/S1350482703002081>

**Publisher's Note** Springer Nature remains neutral with regard to jurisdictional claims in published maps and institutional affiliations.